HHS Public Access

Author manuscript

Org Biomol Chem. Author manuscript; available in PMC 2018 October 11.

Published in final edited form as:

Org Biomol Chem. 2016 January 14; 14(2): 389–408. doi:10.1039/c5ob01839k.

Fluorinated porphyrinoids as efficient platforms for new photonic materials, sensors, and therapeutics

N. V. S. Dinesh K. Bhupathiraju[#a], **Waqar Rizvi**[#a], **James D. Batteas**[b], and **Charles Michael Drain**[a,c]

[a]Department of Chemistry and Biochemistry, Hunter College and Graduate Center of the City University of New York (CUNY), 695 Park Avenue, New York, NY 10065, USA

[b]Department of Chemistry, Texas A&M University, College Station, TX 77842, USA

[c]The Rockefeller University, 1230 York Avenue, New York, NY 10065, USA.

[#] These authors contributed equally to this work.

Abstract

Porphyrinoids are robust heterocyclic dyes studied extensively for their applications in medicine and as photonic materials because of their tunable photophysical properties, diverse means of modifying the periphery, and the ability to chelate most transition metals. Commercial applications include their use as phthalocyanine dyes in optical discs, porphyrins in photodynamic therapy, and as oxygen sensors. Most applications of these dyes require exocyclic moieties to improve solubility, target diseases, modulate photophysical properties, or direct the self-organization into architectures with desired photonic properties. The synthesis of the porphyrinoid depends on the desired application, but the de novo synthesis often involves several steps, is time consuming, and results in low isolated yields. Thus, the application of core porphyrinoid platforms that can be rapidly and efficiently modified to evaluate new molecular architectures allows researchers to focus on the design concepts rather than the synthesis methods, and opens porphyrinoid chemistry to a broader scientific community. We have focused on several widely available, commercially viable porphyrinoids as platforms: meso-perfluorophenylporphyrin, perfluoro-phthalocyanine, and meso-perfluorophenylcorrole. The perfluorophenylporphyrin is readily converted to the chlorin, bacteriochlorin, and isobacteriochlorin. Derivatives of all six of these core platforms can be efficiently and controllably made via mild nucleophilic aromatic substitution reactions using primary S, N, and O nucleophiles bearing a wide variety of functional groups. The remaining fluoro groups enhance the photo and oxidative stability of the dyes and can serve as spectroscopic signatures to characterize the compounds or in imaging applications using 19F NMR. This review provides an overview of the chemistry of fluorinated porphyrinoids that are being used as a platform to create libraries of photo-active compounds for applications in medicine and materials.

cdrain@hunter.cuny.edu.

1. Introduction

Porphyrinoids e.g. porphyrins (Pors), phthalocyanines (Pcs), corroles (Cors), chlorins (Chls), bacteriochlorins (Bacs) and isobacteriochlorins (Ibacs) have applications in diverse fields such as medicine,[1] solar energy conversion,[2] optical sensors,[3] electronic devices,[4] supramolecular systems,[5] photovoltaic cells,[6] and catalysis.[7,8] Porphyrinoids are large aromatic dyes that are 1–1.5 nm in diameter. The Por core has 11 π bonds (Fig. 1) and the Pc has an additional 8 in the fused isoindole structure (Fig. 1), Cor and Chl have 10 while Ibac and Bac have 9 each. These macromolecules are the focus of research because of their stability under a wide range of environmental conditions, absorption in the visible and near infra-red (NIR) ranges of the electromagnetic spectrum (400–1000 nm), many derivatives possess long lived triplet excited states that sensitize singlet oxygen ($^1O_2$) formation to potentiate phototoxicity as anticancer and antibiotic agents, and the redox properties of metalloporphyrinoids are used in catalysis.[9–12] These macro-cycles can chelate with nearly every metal in the periodic table which results in variable functional properties such as tuneable excited state lifetimes, redox potentials, catalytic activities, molar absorption coefficients, and molecular dynamics. Functional groups on the periphery of structurally rigid porphyrinoids provide topological diversity, making these dyes well suited for the engineering of supramolecular materials.[9]

Fluorous porphyrinoids are usually more stable towards oxidative degradation,[13-15] have different excited state dynamics because of changes in the HOMO–LUMO energy gap, and exhibit different pharmacokinetics.[16] The perfluorophenyl-porphyrin ($TPPF_{20}$), fluorophthalocyanine (PcF_{16}) and perfluoro-phenylcorrole ($CorF_{15}$) are now commercially available. $TPPF_{20}$ is converted to the corresponding Chl (CF_{20}), Ibac (IF_{20}), and Bac (BF_{20}) compounds (Fig. 1) using Diels–Alder and 1,3-dipolar cycloaddition reactions.[17–19] Compared to Por, Chl, Ibac, and Bac have NIR absorbance but still show high $^1O_2$ yield for PDT.[17] These fluorinated porphyrinoids can be used as ^{19}F magnetic resonance imaging (MRI) agents for *in vivo* imaging in combination with fluorescence spectroscopy.[20–22] These molecules are strongly stabilized due to the high electro-negativity of fluorines (Pauling electronegativity[23] for F = 3.98). For Pcs, in particular, the electron-withdrawing halogens tend to lower the LUMO, which makes the molecule more stable to ambient oxidation.[24]

Despite the aforementioned advantages of fluorous porphyrinoids, many applications are hampered by poor solubility and/or processability. For example, insolubility in water and no selectivity towards disease hamper their use as therapeutics, while amorphous aggregation limits photonics applications. *De novo* synthesis of all but the simplest porphyrinoids results in low yields, which impedes facile assessments of derivatives in materials and medicine.

N,N-Dimethylformamide (DMF), acetonitrile, chloroform, and toluene are common solvents for metallation of the free base Por.[25] In 1990, Kadish *et al.*,[26] in an attempt to metallate *meso*-$TPPF_{20}$ in DMF, obtained *meso*-tetrakis(2,3,5,6-tetra-fluoro-4-(dimethyamino)phenyl)porphinato metal complexes. Refluxing $TPPF_{20}$ in DMF without the metal salt also resulted in the dimethylamino substituted Por. The trace dimethylamine formed at high temperatures is nucleophilic enough to replace the *p*-fluoro group *via* a

nucleophilic aromatic substitution reaction. This opened a new avenue for research using fluorinated porphyrinoids as platforms to develop new dyes for diverse applications.

In 1991, Mansuy and co-workers[27] studied the nucleophilic substitution reaction on the free base and metal analogues of $TPPF_{20}$ including one with bromine on β-pyrrolic positions. They used S, N and O nucleophiles with electron donating functionality and observed higher yields of tetra substituted products with selective substitution on all four *p*-fluoro positions. But in the case of nucleophiles with electron withdraw-ing functional groups they observed complex mixtures. Later, lithium organic compounds were used by Kalisch and Senge to successfully substitute the Por core using the same reaction.[28,29] This substitution usually takes place *via* a two-step addition–elimination reaction mechanism in aprotic solvent using amine,[26,30] thiol,[31–34] or hydroxy[35–38] groups as nucleophiles. Boyle and co-workers reported the substitution chemistry of mono-(pentafluorophenyl)porphyrin containing different thiol functional groups. Both one step and two step reactions were reported. Thiols were added to mono-(penta-fluorophenyl)-porphyrin in DMF/Et_3N (one step reaction)[32] or mono-(pentafluorophenyl)porphyrin was reacted first with Na_2S and then with a range of electrophiles, where a transient thiolate intermediate was obtained *in situ* to give a thio tether link (two step reaction).[34] For $TPPF_{20}$ the *p*-fluorine atom is selectively substituted prior to the *o*-or *m*-fluorines,[22] but the *m*-position can be substituted with greater equivalents of the nucleophile and elevated temperatures. Thiols result in high yields and take less time compared to amines and hydroxyls. The nucleophile softness dictates the efficiency of the substitution in the order: S > N > O (Fig. 2).[39,40] Both the free base and the metallo fluorinated porphyrinoids are suitable for substitution chemistry, or the dyes can be metallated post modification. By controlling the stoichiometry and reaction conditions, the $TPPF_{20}$, CF_{20}, IF_{20} and BF_{20} platforms can be appended with 1–4 groups.[33,41] Note that asymmetric moieties appended onto the CF_{20}, IF_{20} and BF_{20} platforms result in diastereomers at the bridge head positions. Because of the orthogonal geometry of the aryl groups and the barrier to rotation, substitution of more than one *m*-position results in atropisomers. The PcF_{16} can be appended with 1–16 groups.[42]

For example, several biomolecules such as sugars, polyamines, polyethylene glycols (PEG), peptides, amino acids, and boron clusters have been appended to one or more of the fluorous dyes for disease targeting.[41,43–47] There are few examples where more than one biomolecular motif (*e.g.* cell targeting, hydrophilic, or chemotherapeutic) can be appended to a dye but the molecular topology of the porphyrinoids allows a range of substitutions.[41,46] For biotargeting and bio-sensing, the multiple valence significantly increases binding to the target. Other strategies that exploit the topological richness of the porphyrinoids are as drug carriers, *e.g.* boron clusters for boron neutron capture therapy (BNCT).[41,46] A variety of alkanes can be appended to drive self-organization into nano-scale thin photonic films and/or to manipulate the photo-physical properties of the dyes leading to a more effective application in materials such as solar energy harvesting.[42,48–51] Appending exocyclic motifs onto the redox active metalloporphyrinoids results in molecules and materials with improved catalytic properties for organic transformations.[52,53] This review will focus mainly on the nucleophilic substitution of fluorine analogues belonging to Pors, Pcs, Chls, Cors, Bacs and Ibacs. We will discuss their physicochemical as well as biomedical and material properties and applications.

2. Substituted fluorinated porphyrinoids for biological applications

Porphyrinoid based photosensitizers (PS) have been used in medicine for treating various types of diseases (oncology and non-oncology) such as bladder, brain, breast, skin, lung, esophagus, and bronchial cancers,[54,55] age-related macular degeneration, cardiovascular disease, ophthalmic disease, hair growth, acne, and psoriasis using photodynamic therapy (PDT).[56–62] These PS are presently studied for their application in treating microbial infections (bacterial, fungal, parasitic, and viral infections) using photodynamic antimicrobial chemotherapy (PACT).[55,63–66] These PS have also been used to diagnose the above mentioned diseases and so are considered to be effective theranostic (imaging and treatment) agents.

PDT treatment involves three important elements: PS, which should accumulate specifically in the targeted site, triplet oxygen, and light. For PDT, the patient is administrated a non-toxic PS dye. After sufficient time for maximum drug uptake by the cancer cells, the tumor is selectively irradiated with light to result in cytotoxic reactive oxygen species, which results in tumor destruction.[54] Presently there are few approved PDT agents (Photofrin, protoporphyrin IX, *meso*-tetra-hydroxyphenylchlorin (*m*-THPC), and verteporfin) to treat several diseases.[54,67] These porphyrinoid based PS have several disadvantages such as poor water solubility, poor light absorption in NIR, poor disease selectivity and light sensitivity after treatment. Other treatment methods such as BNCT involving carboranes and porphyrinoids were also studied, where por-phyrinoids were used both as imaging agents and as an adjunct treatment (PDT) method.[68,69]

Important ongoing approaches for improving the potency of PS are fluorinated derivatives that modulate pharmaco-kinetics, $^1O_2$ production, photostability, and lipophilicity. In addition to the intrinsic fluorescence of the porphyrinoids, magnetic resonance of fluorinated compounds (^{19}F-NMR),[70–72] ^{18}F positron emission topology (PET) imaging,[13,73] carbon–fluorine spectroscopy (CFR),[16] and fluoro-Raman spectroscopy (FRS)[74] are all enabled for sensitive and minimally invasive imaging of disease or as sensors.

Another advantage of these porphyrinoid platforms is the ease of substituting multiple copies of exocyclic biotargeting motifs to exploit multivalency effects, or several different motifs to direct the dyes to different targets.[16] In this section we discuss the nucleophilic substitution of various bio-motifs on fluorinated porphyrinoids for medical applications.

2.1. Porphyrins

Marzilli and co-workers reported the synthesis of 5,10,15,20-tetrakis[2,3,5,6-tetrafluoro-4-(2-trimethylammoniumethyl-amine)-phenyl]porphyrin *via* nucleophilic substitution of dimethyl-1,1-ethylenediamine for DNA binding studies.[30] Boyle and co-workers reported a water soluble Por containing three glucose moieties substituted on *para* positions of the perfluorophenyl group and a positively charged *N*-alkyl-pyridyl moiety *via* nucleophilic substitution (see Fig. 3).[75] These compounds were then studied on human colorectal adenocarcinoma (HT29) cells for their PDT activity. Comparison of LD_{90} (concentration required to kill 90% of cells) showed that 5-(*N*-octa-decyl-pyridyl)-10,15,20-tris(4-

thioglycosyl-2,3,5,6-tetrafluoro-phenyl)porphyrin had the best phototoxicity (irradiated with red light) along with low dark toxicity (absence of light).

In 2001, we reported the synthesis of a symmetrical sugar substituted $TPPF_{20}$ *via* nucleophilic substitution of thioglucose and thiogalactose to obtain PGlc4 and PGal4 (Fig. 4)[76] in high yield. These compounds were then tested on the cancer cell line (human breast cancer cells (MDA-MB-231), and rat fibro-blasts (normal (3Y1), partially transformed (3Y1c-Src), and fully transformed (3Y1v-Src))) for their uptake and PDT efficacy.[31] Among the two conjugates $PGlc_4$ showed high cell uptake and better PDT efficacy compared to $PGal_4$. When $PGlc_4$ was studied for its uptake in normal cells (rat fibroblast 3Y1) vs. cancer cells (rat fibroblast 3Y1c-Src and 3Y1v-Src) there was higher uptake in the 3Y1v-Src cell line, intermediate uptake in the 3Y1c-Src cell line and no uptake in the 3Y1 cell line. These studies suggested that sugar appended porphyrinoids show selectivity towards cancer cells compared to normal cells.

Hirohara and co-workers extended the study by comparing the Zn(II), Pd(II) and Pt(II) complexes of $PGlc_4$ with the free base $PGlc_4$ (Fig. 4) for their phototoxicity.[77] Here, they started with the free base $TPPF_{20}$ and metallated it with Zn, Pd and Pt before carrying out the nucleophilic substitution of acetyl protected thio-glucose in the presence of diethylamine (DEA) as base and DMF as solvent at room temperature. The final step was deprotection of acetate groups. The human epithelial (HeLa) cell line was used to test the phototoxicity of these com-pounds. Zn(II) and Pd(II)$PGlc_4$ showed high phototoxicity due to the heavy-atom effect. Surprisingly, Pt(II)$PGlc_4$ showed a low phototoxicity. The same group also studied the effect of substi-tution patterns on the phototoxicity of glycosylated Pors. They similarly carried out the synthesis of five possible S-glucose (mono-, 5,10-di-, 5,15-di-, tris-and tetrakis-) substituted Pors (Fig. 4).[33] Cell uptake and phototoxicity studies of these conjugates were carried out using the HeLa cell line. Among these conjugates, the 5,15-di-substituted glucose Por showed the highest cell uptake and phototoxicity.

Cavaleiro and co-workers reported several glycosylated Pors and studied their significance for antiviral activity against herpes simplex virus types 1 and 2 in Vero cells. They synthesized mono substituted *O*-galactosylPor (Fig. 5)[78] via nucleophilic substitution of isopropylidene protected O-galacto-pyranose on $TPPF_{20}$ using the NaH base, followed by de-protection of isopropylidene. This compound showed very good antiviral activity even at lower than maximum noncyto-toxic concentration.

In 2006, our group studied the substitution of aminoPEG, ethylenediamine, and lysine groups on to $TPPF_{20}$ (Fig. 6) under microwave irradiation, yielding the symmetric tetra substituted Por in quantitative yields.[79] In this study, we used *N*-methylpyrrolidine (NMP) as solvent without any base. Conventional heating at 60–70 °C takes more than 20 hours with six different possible products while microwave reaction took less than 30 minutes with only tetra substituted products.

Král and co-workers reported the synthesis, cell uptake and phototoxicity studies of glycol Pors (Fig. 7).[45] In their study they substituted *O*-glycols and aminoethanol on the $TPPF_{20}$. The DMF solvent and the NaH base were used to substitute the *O*-glycols. They obtained

moderate yields of tetra substituted products as the reaction was carried out at low temperatures and hard nucleophiles such as oxygen require heating for better yields. Then for the substitution of aminoethanol they used dioxane as solvent with no base at 150 °C to obtain the tetra amino substituted product with the free –OH group in high yields. This shows that soft nucleophiles preferentially substitute the fluorine in the presence of harder nucleophiles. The hydroxy terminated Pors exhibited a better intracellular uptake and phototoxicity compared to methoxy terminated derivatives when tested *in vitro* on human promyelocytic leuke-mia (HL60) and mouse mammary carcinoma (4T1) cell lines and *in vivo* on NuNu mice bearing human breast carcinoma MDA-MB-231.

Boyle and co-workers reported the synthesis of metallated Ni(II) and Ga(III) and free base tetra substituted thioPEG conjugates in high yields (Fig. 7).[80] These conjugates were evaluated with a human Caucasian colon adenocarcinoma (Caco2) cell line for their phototoxicity efficacy and it was found that PEGs containing higher chain length showed high phototoxicity due to better water solubility compared to Por derivatives containing shorter PEGs. For the Ga(III)Por derivatives, those with longer PEG chains bearing an –OPh axial ligand showed the best phototoxicity results among the nine derivatives studied.

Cavaleiro and co-workers reported the synthesis, cellular uptake, subcellular localization and phototoxicity of mono and tetra substituted O-chalconePor derivatives (Fig. 7).[81] In this study, *O*-chalcone was reacted with $TPPF_{20}$ in the presence of K_2CO_3 as base and DMSO as solvent at 100 °C to obtain derivatives in moderate yields. These compounds were tested on the monkey kidney cell line (COS-7). The tetra substituted derivative showed significant uptake compared to the mono substituted derivative, neither compound was phototoxic, and they localize in the nucleus and/or perinuclear loci. The same group reported the synthesis of porphyrin–quinolone conjugates where they synthesized five Zn(II) complexes (mono-, 5,10-di, 5,15-di, tri, and tetra). *O*-propargyl groups were appended on to $TPPF_{20}$ via nucleophilic substitution followed by metallation (Fig. 8).[36] Then using 1,3-dipolar cycloaddition reaction, they conjugated 6-azidoquinoline on to preformed Zn(II) complexed *O*-propargylPors to yield five Por– quinoline derivatives in quantitative yields.

Král and co-workers reported the synthesis of Por–β-cyclodextrin (β-CD) or γ-cyclodextrin (γ-CD) conjugates (Fig. 9). They also conducted binding studies of several chemotherapy drugs with cyclodextrin (CD) for versatile drug delivery and *in vitro* and *in vivo* studies.[82] Binding studies revealed that doxorubicin has good binding affinity towards Por–γ-CD 3 and paclitaxel has good binding affinity towards Por–β-CD conju-gates 1, 2 and 4. Supramolecular carrier–chemotherapy drug complexes were then tested in vitro using 4T1 and human chronic myelogenous leukemia K562 cell lines, and in vivo using BALB/c mice transplanted with 4T1 cells. These studies reveal that combination therapy (PDT and chemotherapy) can be used as an efficient method to treat cancers.

Cavaleiro and co-workers reported the synthesis and $^1O_2$ studies of Por–phosphoramidate conjugates (Fig. 10).[83] They carried out nucleophilic aromatic substitution of aminoalkyl phosphoramidates (different alkyl chain lengths) onto $TPPF_{20}$ to obtain mono and tetra substituted porphyrin–phosphorami-date conjugates. Among these conjugates tetra substituted porphyrin–phosphoramidates showed higher $^1O_2$ values and among the tetra

substituted derivatives, the porphyrin–phosphoramide with a butyl chain (n = 4) showed the highest $^1O_2$ value.

Tomé and co-workers reported the synthesis of tetra cat-ionic Pors (Fig. 11) and studied their activity against fungal conidia (antifungal activity).[84] In this study, 4-mercapto-pyridine was substituted on $TPPF_{20}$ using DEA as base at room temperature to yield tetra substituted mercaptopyridylPor. Sulphur, being a softer nucleophile than nitrogen, undergoes nucleophilic substitution under these mild conditions. Additionally, iodomethane and 1-iodopentane were reacted respectively to obtain tetra cationic Por derivatives. Com-pounds were tested on *Penicillium chrysogenum* conidia strain. Among these cationic derivatives tetramethylpyridyl cationic Por showed better photodynamic inactivation. Recently, they reported cationic Pors with inverted pyridinium groups (Fig. 11)[85] where they reacted 4-hydroxypyridine with $TPPF_{20}$. Nitrogen, being a softer nucleophile than oxygen, is observed to undergo substitution and tautomerize to the pyridone form. On further reaction with DMSO, cationic methoxypyridyl-porphyrin was obtained.

Recently, Vicente and co-workers published the synthesis and *in vitro* studies of carboranePor derivatives containing three *p*-carborane and cancer targeting units such as polyamines, glucose, peptide and amino acid. In addition, symmetric Pors containing four p-carborane units for applications in BNCT and/or PDT (Fig. 12) were reported.[41,46] Symmetric tetra substituted porphyrin–*p*-carborane was obtained in quantitative yields. The PEG derivative was further conjugated to peptide (YRFA) and amino acid (lysine) via an amide coupling reaction. Phototoxicity, dark toxicity, cell uptake, localization and in vitro BBB studies were carried out on all these conjugates. None of the conjugates showed dark toxicity when tested on the human glioma T98G cell line and the polyamine, spermine, conjugates are the most taken up by these cells and the most phototoxic. Human carcinoma HEp2 cell line studies showed that polyamine conjugates were mainly localized in the Golgi, endoplasmic reticulum, and mitochondria while the glucose conjugate was localized in mitochondria and lysosomes. Arginine and peptide (YRFA) localize in the Golgi, lysosomes, and mitochondria. Moderate permeability of these compounds was observed when *in vitro* blood brain barrier (BBB) studies on human brain capillary endothelial hCMEC/ D3 cells were conducted. The low dark toxicity and good phototoxicity for some of the polyamine conjugates reveal that these compounds could be promising agents for treating cancers with BNCT and PDT combined.

2.2. Chlorins, isobacteriochlorins and bacteriochlorins

One way to improve the cancer diagnostics potential and PDT efficacy of porphyrinoids (e.g. by treating deep tumor tissues) is to enhance the NIR absorption bands.[86-88] Chl, Ibac, and Bac are considered promising PS due to a strong NIR absorption and minimal dark toxicity. Chls are derivatives of Pors with one double bond on the pyrrole missing, Ibac are missing two double bonds on adjacent pyrroles and Bacs are missing two double bonds on opposite pyrroles. CF_{20}, IF_{20} and BF_{20} (Fig. 1) synthesis from $TPPF_{20}$ was reported by Cavaleiro and co-workers.[17]

Vicente and co-workers utilized the CF_{20} to substitute 1-mercapto-*o*-carborane (Fig. 13).[68] This compound showed no dark toxicity and was localized in cell lysozymes when tested

using the HEp2 cell line. Fluorescence microscopy studies revealed that this compound is mostly found in the cyto-plasmic membrane when tested using B16F1 melanotic mela-noma cells. *In vitro* and in vivo results suggest that this compound can be used as a PDT agent in conjunction with BNCT.[69] Kalinin and co-workers reported the synthesis of boronated Chls and Pors *via* the regioselective substitution of lithiocarboranes onto $TPPF_{20}$ and CF_{20} (Fig. 13).[89]

We reported the synthesis of three nonhydrolysable tetra-thioglycosylated porphyrinoids ($CGlc_4$, $IGlc_4$, and $BGlc_4$).[90] Hir-ohara and co-workers reported the synthesis and *in vivo* studies of S-glucose and S-galactose substituted Chl derivatives (Fig. 14).[91] These glucose and galactose chlorin derivatives were synthesized via nucleophilic aromatic substitution of acetyl protected S-glucose or acetyl protected S-galactose onto CF_{20} followed by deprotection. In vitro studies of $CGlc_4$ and $CGal_4$ are compared with previously reported $PGlc_4$ and $PGal_4$ [31] using the HeLa cell line. Both $CGlc_4$ and $PGlc_4$ showed continuous uptake up to 24 hours while the other two compounds reached a plateau after 12 hours.

We reported the photophysical properties and *in vitro* studies of $CGlc_4$, $IGlc_4$, and $BGlc_4$ (Fig. 14).[92] $CGlc_4$ and $IGlc_4$ have stronger and redder absorption bands compared to $PGlc_4$ and increased fluorescence quantum yield by 6-and 12-fold, respectively, in phosphate buffered saline (PBS). $BGlc_4$ has the lowest energy Q-band and is considerably red shifted to 730 nm with nearly 50-fold greater absorbance but the fluorescence quantum yield is similar to $PGlc_4$. Fluorescence imaging studies of these conjugates using MDA-MB-231 and mouse embryonic fibroblast cells K:Molv NIH 3T3 reveal that these compounds are taken up by cancer cells. These com-pounds were also studied for two photon fluorescence imaging on Chinese hamster ovary cells and we found that $IGlc_4$ has good two photon absorption (TPA) between 760 and 880 nm, and the cross section is 24.5 GM at 860 nm.[93]

Hirohara and co-workers then reported the synthesis of Pd(II) complexes of $CGlc_4$ and studied the *in vitro* photocytotoxicity (Fig. 14).[94] As expected from numerous prior studies,[95,96] the presence of the heavy atom Pd(II) enhances the singlet oxygen quantum yield. However, they found that the free base $CGlc_4$ has higher *in vitro* photocytotoxicity compared to the Pd(II) complex using HeLa, metastatic B16-BL6, weakly metastatic B16F1, and metastatic 4T1 cell lines. Then, Morita and co-workers used xenograft tumor models to compare the PDT efficacy of $CGlc_4$, the non-glycosylated conjugate (CF_{20}), and aspartyl chlorin (NPe_6) using several different human cancer cell lines.[97] $CGlc_4$ showed a better PDT efficacy and suppressed tumor growth with no side effects.[98]

Recently, Brückner and co-workers reported the nucleo-philic substitution reaction of thioPEG with different chain lengths onto *meso*-tetrakis(pentafluorophenyl) oxazolochlorins to obtain tetra substituted pegylated oxazoloChl.[99]

2.3. Corroles

Cors are porphyrinoids with potential use as PS. Cors are tetra-pyrrolic macrocycles with 18 π conjugated electrons but with one less *meso* carbon and stabilize +3 metal ions.[100] Cors have larger optical cross sections in the red compared with Pors due to stronger Q absorption bands between 450 nm and 650 nm. Cors can have high $^1O_2$ generation quantum efficacy,[101]

thermal and photochemical stability,[101] and can be metabolized faster *in vivo*.[101,102] Cors are extensively studied as new generation PS for applications in PDT.[39,103]

The first synthesis of fluorinated Cor and water soluble pyridyl substituted fluorinated Cor derivatives was reported by Gross and co-workers.[100,104] In 2007, our group explored the substitution chemistr on fluorinated Cor ($CorF_{15}$) with acetate protected glucose, xylose and thiopyridine.[39] When thio-glucose and thio xylose were mixed with $CorF_{15}$ a library of six different products was observed as expected. An attempt to make a library of 18 compounds by mixing $CorF_{15}$ with thio-glucose, thioxylose and thiopyridine resulted in only 17 (Fig. 15). From this study, we also observed that due to an increase in the acidity of Cor compared to Por, the substitution is somewhat slower and the NMP solvent is best for the substitution of nucleophiles on Cor. The higher acidity is because of three NH pyrroles compared to two in Por. Barata and co-workers reported the substitution of the protected *O*-glycosyl moiety on CoF_{15},[105] resulting in mono substituted products with two positional isomers (Fig. 15). *In vitro* uptake and phototoxicity studies of these compounds using human acute T cell leukaemia cells (Jurkat cells) were carried out. There was good cell uptake but a low phototoxicity.

Osuka and co-workers reported the synthesis of both mono and tri substituted derivatives of fluorinated Cor *via* nucleo-philic substitution of several amines (primary and secondary) with moderate to high yields (Fig. 16).[106] Recently, Schoefberger and co-workers reported both metallated and free base amino acid conjugates of CoF_{15} (Fig. 17).[107] Thiazine ring formation was observed when CoF_{15} was reacted with cysteine. This is due to the presence of nucleophiles S and N on the amino acid. The reaction was carried out using a strong base (NaH) and heat in DMSO. Due to these harsh conditions the softer S nucleophile reacts first, replacing the *p*-fluoro group, followed by N reacting at *meta* position, forming a stable six membered thiazine ring.

2.4. Phthalocyanines

Pcs are chemically stable, and have a strong absorption peak in the NIR region of the optical spectra ($\lambda_{max} \approx 670$ nm, $\varepsilon \approx 10^5$ L mol^{-1} cm^{-1}) where light penetrates deeper into tissues and have good $^1O_2$ quantum yields.[108–110] Due to these properties, extensive research has been conducted on their synthesis and functionalization to tune their photochemical and photophysical properties.[111] The disadvantages of these porphyrinoids include difficulties in purification, formation of isomeric mixtures, and strong aggregation. To solve these issues, presently research studies focus on fluorinated ana-logues.[16] Several bio-motifs containing S, N, and O groups can be easily substituted using click substitution chemistry to obtain pure Pcs with better water solubility. Our group was the first to report the synthesis of a zinc phthalocyanine (ZnPc) appended with eight nonhydrolysable thioglucose units obtained *via* nucleophilic substitution of acetyl protected thio-glucose onto commercially available $ZnPcF_{16}$ (Fig. 18).[112] Fluore-scence microscopy of this compound on the MDA-MB-231 cell line showed a very good uptake but the compound aggregated, resulting in quenching of fluorescence. Slow disaggregation of the glycolPc inside the cell or tissue may allow these compounds to be used diagnostically or therapeutically.[67]

Tomé and co-workers reported the synthesis and photophysical properties of glycodendritic conjugates of Pors and Pcs bearing eight and sixteen Dgalactopyranose units on triazine linkers, respectively (Fig. 18).[113] When $^1O_2$ studies were conducted, high quantum yields were observed, suggesting the potential as PDT agents. Recently, *in vitro* studies of a hexa-deca-galactoPc dendrimer (Fig. 18) were carried out on two different human bladder cancer cell lines, UM-UC-3 and HT-1376, for their PDT efficacy.[114] They observed no dark toxicity, high cell uptake, and high phototoxicity. These results were attributed to the presence of galectin-1 and GLUT1 receptors on the two aforementioned bladder cell lines. The same group synthesized the cationic octa substituted thiopyridyl Pc (Fig. 18) *via* nucleophilic substitution of thiopyridine on $ZnPcF_{16}$ followed by methylation. The product was obtained in quantitative yields.[115] Antiviral PDT activity was studied on this compound but did not show promising results.

Recently, Tomé and co-workers reported Pc–CD conjugates (Fig. 19) for cancer PDT.[116] Three such derivatives, Pc–α-CD, Pc–β-CD and Pc–γ-CD, were synthesized *via* nucleophilic substitution of cyclo-maltohexaose (α-CD), cyclo-maltoheptaose (β-CD) and cyclo-maltooctaose (γ-CD) on two fluorine atoms of PcF_{16}. Then, they tested these compounds on the UM-UC-3 bladder cancer cell line for phototoxicity and the results revealed that Pc–α-CD and Pc–γ-CD exhibited higher phototoxi-city compared to Pc–β-CD.

2.5. Triply bridged fused porphyrin

Current FDA approved PS have one-photon absorption peaks in the visible region (400 nm to 650 nm).[54] Dyes that have stronger absorption cross section in the NIR region such as Chl, Bac, IBac, Pc, and Por dimers were also prepared[90,112,117] for the treatment of deeper seated tumors.[118] Recently, research has been carried out on two-photon absorption (TPA) dyes that absorb two lower energy photons simultaneously to arrive at the same excited state as single photon absorptions. These TPA dyes have absorption bands in the NIR or infrared region (800–1100 nm), so scattering of these wavelengths in tissues is much less than for higher energy photons.

Osuka and co-workers reported that hexakis(pentafluorophenyl) substituted *meso–meso*-linked Zn(II) diporphyrin has little fluorescence, but a good TPA and good $1O_2$ quantum yield.[119] However, this compound is neither soluble in aqueous media nor specific towards diseased tissues for medical applications. Our group recently reported the synthesis and phototoxicity of the hexathioglucose derivative of the triply bridged fused Por dimer (Fig. 20).[47] This compound showed good $1O_2$ quantum yield (0.78 ± 0.03) in DMSO. *In vitro* phototoxicity studies carried out on the MDA-MB-231 breast cancer cell line showed significant cell death (IC_{50} = 13 μM), in agreement with $^1O_2$ results when white light was exposed for 20 min, and after 24 hours 75% of the cells were necrotic. No dark-toxicity was observed.

3. Substituted fluorinated porphyrinoids for application in materials

The tremendous potential applications of Por, Pc and Cor derivatives come from their photophysical and electrochemical properties, remarkable stability, and ability to chelate to

nearly every metal to further diversify the chemical properties. These applications include catalysis,[52,120–125] solar energy harvesting dyes,[3,35,71,127-130] sensors,[38] and tracers. The multifunctional properties are modulated by appending various chemical moieties on the periphery of the macrocycles using nucleophilic aromatic substitution chemistry and by varying the core metal. As photonic materials, the exocyclic motifs can be used to dictate the supramolecular organization of the dyes, which determines the efficiency of energy or electron transfer, determines the hierarchical order of films, and affords opportunities for molecular recognition of analytes. While metalloPors can be good catalysts and excellent sensors, Cors have been employed as environmental tracers. Porphyrinoid based solar energy harvesting devices have also been extensively studied.

3.1. Catalysis

Over the last few decades, many research groups have reported that synthetic metalloPors can be efficient and selective catalysts for various oxidation and reduction reactions.[120,131–134] Pors with Fe, Mn, Co, and other metal ions have been used as catalysts in laboratory-scale reactions using a variety of oxygen sources.[135] Such catalytic reactions can mimic the activity of cytochrome P450 monooxygenation reactions.[52] The efficiency and catalytic activity of metalloPors depend on a few variables: the temperature, pressure, solvent, source of oxidant, axial ligand, and the structure of the substrate. These catalysts are observed to be effective in homogeneous systems. Hydrocarbon epoxidation and hydroxylation are typical products of these reactions.[120] A variety of oxygen donors ranging from molecular oxygen to peroxides, peracids, and iodosylbenzene are used for these reactions.[136] Due to ease, availability, cost and a greener approach, molecular oxygen in air is preferable as an oxygen donor because no energy is used to manufacture and store it.

However, there are a few drawbacks of these catalysts as secondary reactions deactivate the catalytic species, often leading to low turnover number (TON). Self-oxidative degradation during the catalytic process is a key issue that limits the use of metalloPor as catalysts. To overcome this, electron withdrawing groups such as fluorines or bulky substituents are often appended to the Por macrocycle.[137,138] The fluorous porphyrinoid platforms allow facile substitution chemistry to append exocyclic moieties that modulate catalysis. Supramolecular Por catalysts are designed to prevent self-oxidative degradation and to enhance substrate selectivity for quicker catalysis and better TON.[52,53] To minimize oxidative damage and to develop metalloPors[139–143] with more robust structures, our group prepared aggregated metalloPors into organic nanoparticles (ONP).[52,53]

McKeown and co-workers[124] have reported that hydroquinone oxidation catalytic activity is enhanced in a spiro-linked porphyrinoid polymer network. There was a significant difference seen in comparison to the small molecular mass derivative for H_2O_2 decomposition, cyclohexene oxidation and hydroquinone oxidation. These materials mimic the biological systems in which the rigid spiro-linked network creates space around the active sites which allows the substrate to gain access and the reaction to take place. There is definitely a potential for heterogeneous catalysis of network polymers of intrinsic microporosity (PIMs) with catalytically active units incorporated within.

Breslow and co-workers[125] used the simple click-type chemistry to append β-CD onto the $TPPF_{20}$ macrocycle (Fig. 21). In this case the β-CD behaves as an artificial binding pocket for catalysis while the natural Por core catalytic properties are retained. They reported that fluorines on the phenyl rings stabilize the Por against autooxidative destruction. This stability results in a high TON and the appended β-CD provides substrate and regio/stereoselectivity in the hydroxylation of steroid substrates.

George and co-workers[122] reported Por derivatized with fluorous 'ponytails' as biphasic catalysts (Fig. 21) to achieve photo-oxidations in supercritical carbon dioxide with $1O_2$. This study revealed that the fluorinated Por photocatalyst can be recycled 10 times. This is a dramatic increase in catalyst stability compared to previous studies.

Nakagaki and co-workers[121] have reported ethylene glycol substitution onto the core $TPPF_{20}$ platform (Fig. 21) and found that *p*-fluorines on the *meso*-aryl groups substitute preferentially. After metallation of the free-base macrocycles with iron and manganese, these materials were immobilized on layered double hydroxide (LDH) and silica supports. These materials are found to be catalytically active in the oxidation of (*Z*)-cyclooctene and cyclohexane by iodosylbenzene. The stability of the materials allowed their reuse for at least three additional cycles of (*Z*)-cyclooctene oxidation. Earlier this year, the same group[120] reported on substituting galactodendritic moieties onto the core $TPPF_{20}$ platform (Fig. 21). The supported Cu(II) and Zn(II) complexes are catalytically active towards the oxidation of alkenes, alcohols, and catechol and can be reused.

Our group[52,53] has published a green chemistry approach to develop ONP from substituted metalloPors for oxidative catalysis of olefins and alkenes. These 10–30 nm ONP are easily formed by injecting the metalloPor into a host solvent such as DMSO or DMF into water while vigorously mixing. Since water is the primary solvent (ca. 95%) and the ONP activate molecular oxygen in air, these catalysts avoid halogenated solvents or toxic oxygen sources such as iodosylbenzene. The energy requirements are minimal because the reactions are run at ambient temperature and pressure. We appended highly fluorinated alkyl groups on the *para* positions of the core $TPPF_{20}$ (Fig. 21). Oxidative catalysis studies on cyclohexene with various Fe(III) and Mn(III) metalloPors show that the rate of oxidation by the ONP is much slower than the solvated compounds, but the TONs are 10–50-fold greater. An onion peel mechanism was proposed to explain the slow reactivity and increased TON for these ONP, where only the outer layer of Por is available for the oxidative process, and when these are oxidatively compromised, they exfoliate to expose the next catalytically active layer.

Superoxide (SO) anion radical has dramatic damaging effects on living organisms. The main biological defence system to mitigate SO is superoxide dismutase (SOD) enzymes.[144,145] SODs are enzymes that catalyse the dismutation of SO to hydrogen peroxide and oxygen very efficiently. SOD contains a redoxactive metal with the capability of oxidizing and reducing SO. The endogenous SOD may not be sufficient to remove the highly produced SO under some therapeutic conditions, but direct injection of these enzymes as pharmaceutical agents has problems in terms of stability, immunogenicity and bioavailability.[134] These problems invite research to develop stable and non-toxic low molecular weight SOD mimics for therapeutic applications.

Gross and co-workers[134] reported that metal complexes such as Mn(III) or Fe(III) Cors[146,147] (Fig. 22) catalyze the dismutation of SO. Fe(III) and Mn(III) complexes of the 3,17-bis-sulfonated Cor have been found to be excellent catalysts for the decomposition of peroxynitrite.[134] The p-fluorines have been substituted with methoxy groups to enhance the stability and solubility of these Cors.[134] The Fe(III) Cor derivative is found to be more reactive than the Mn(III) complex. The reactions of metalloCors start with the reduction of SO rather than oxidation

3.2. Sensors

The last 40 years have witnessed an explosive growth in developing sensors and biosensors as portable and economical tools in analytical chemistry. The strong colours, fluorescence, electrochemical activity, stability, and ligation properties of fluorinated porphyrinoids enable them to be the functional heart of sensors.[130] The fluorous porphyrinoid platforms facilitate substitution chemistry to append ligands of choice onto the macrocycle to recognize and report on a diverse array of analytes.

Anions play crucial roles in a number of chemical, biological and environmental processes.[148,149] Diseases such as osteoporosis, Alzheimer's, and cystic fibrosis are caused by perturbations in anion fluxes across cell membranes.[150-152] Anions including cyanide and arsenate are considered a threat when present in the environment, which leads to a need for systems capable of controlling and monitoring these species.[153] MetalloPors with metals such as zinc, rhodium, silver, gold or copper can be used as cyanide sensors because of the essential affinity of cyanide to these metals.[130]

The environmental and biological importance of anions accounts for the critical need for a sensor design to effectively detect these species. Amines and polyamines,[154] calix-pyrroles,[155] subphthalocyanines,[156] Cors,[157] and Pors[158] are used to create anion receptors. Anion recognition involves the NH groups of the pyrrole units in Pors. However, with the discovery of substitution chemistry on these macrocycles, recognition can take place outside the macrocycle. Due to sterics, the inner NH groups are less effective hydrogen bond donors compared to the substituents on the periphery of the macrocycle. For instance, several Pors bearing NH groups at the *ortho* positions of *meso*-aryl substituents have been demonstrated to be effective anion sensors.[158] Pors bearing substituents at the *para* position of the *meso*-aryl groups can also be used for anion recognition. $TPPF_{20}$ can be used as a platform to build new polyamine anion hosts that are effective receptors for dihydrogen phosphate in organic media.[152] Tomé and co-workers[152] have substituted various diamines onto the core $TPPF_{20}$ platform for the development of phosphate anion sensors (Fig. 23). These sensors are reported to interact prefer-entially with phosphate anions both in organic solutions and in basic aqueous media when coated on gold piezoelectric quartz crystals.

Recently, Bruckner and co-workers[130] showed pyrrole-modified Pors bearing a lactone functional group at the macrocycle periphery as optical cyanide sensors. Nucleophilic attack of the cyanide onto the lactone moiety is proved to be the sensing mechanism. A change in the hybridization of the carbonyl carbon couples electronically to the macrocycle and results in a 100 nm red-shifted absorbance band and the Soret band decreases in intensity upon cyanide addition. Substitution of the *p*-fluorine on the pentafluorophenyl moiety with PEG

groups leads to water-soluble derivatives allowing for cyanide sensing in purely aqueous solutions.

Dissolved oxygen (DO) is related to water quality, medicine, food freshness, respiration and metabolism in living organisms, and many other biological applications.[159–161] Mechanism such as fluorescence quenching, oxygen pressure and electrochemistry are used to develop oxygen sensors.[35,160–164] Pt(II) and Pd(II) Pors[156,166] are typical chemical materials acting as fluorescence-based oxygen sensors because of their long triplet state, variable lifetimes from a few to tens of micro-seconds and respectable triplet–triplet energy transfer from these compounds to oxygen molecules. When this energy transfer takes place, the emission intensities and the lifetimes of these sensors are shortened. Pt(II)$TPPF_{20}$ is an excellent sensor because of its good response to oxygen concentrations and high photostability compared to other chromo-phores.[167,168] Meldrum and co-workers[35] reported the synthesis of a new sensor for DO. Simple click-type substitution chemistry was used on the Pt(II)$TPPF_{20}$ platform. The resulting sensor carries four cross-linkable methylacrylate functional moieties (Fig. 23) which can be polymerized and cross-linked with other monomers for polymer sensing films. The sensor was then linked to hydrophilic poly(2-hydroxyethyl-methacrylate)-*co*-polyacrylamide (PHEMA) and hydrophobic polystyrene (PSt) films. The long fluorescence life time and sufficient triplet–triplet energy transfer between the porphyrinic based sensors and oxygen molecules result in a decrease of the oxygen sensors' emission intensities and a shortening of their lifetimes.

Recently, Pcs, coumarin derivatives,[169] and naphthalo-cyanines[170] have been used as fluorescent markers for petroleum fuel derivatives. These compounds are not visible with the naked eye under visible light. However, because of the large optical cross sections and fluorescent properties, they can be easily detected by UV light. In this case, some characteristics of efficient fluorescent markers include (1) good fuel solubility; (2) ambient light invisibility; (3) prolonged shelf-life and stabi-lity; (4) fluorescence emissions in the regions other than those of the fuel itself; (5) cost effective and efficient synthesis on a large scale.[38,171] Porphyrinoids, Pors in particular, are excellent sensor dyes that possess intrinsic photophysical properties that match the requirements for a fuel labelling marker. The desired characteristics for a good fuel labelling system are obtained by substituting non-polar moieties on the commercially available $TPPF_{20}$ platform resulting in "invisible" fluorescent biodiesel markers.[38] Serra and co-workers[38] have reported the substitution of 1-hexadecyloxy-and ethoxy-substituents onto the *p*-fluoro positions of $TPPF_{20}$ (Fig. 23). The developed sensor dyes are soluble in both hydrophobic and hydrophilic environments. The compounds were found to be stable in a biodiesel environment for up to three months. Because of the high stability, solubility and ease of preparation, these markers are reported to be efficient and cost effective.

Cosnier and co-workers[128] have shown the substitution of *p*-fluoro groups on zinc and manganese $TPPF_{20}$ macrocycles with electropolymerizable pyrrole groups (Fig. 23). The electro-oxidation of these metalloPors with functionalized pyrrole groups leads to electrogeneration of polypyrrole films and the electrochemical behaviour of the Pors is retained. The catalytic properties of these materials are associated with the advan-tages

conferred by the electrochemically formed polymers and allow use as a new oxidase based biosensor involving a reduc-tive detection of H_2O_2.

3.3. Solar

Porphyrinoid molecules have great potential applications because of their light absorbing properties. Their stability in harsh environments makes them suitable for applications such as solar energy harvesting. In addition, many of these dyes are low-cost, which makes them suitable for photovoltaic (PV) devices. Pc organic dyes have energy band gaps that are well-matching the incident solar spectrum.[9] However, the use of Pcs in low-cost solar cells faces complications because of poor solubility in organic solvents and narrow absorption bandwidths in the red (Q-band) and ultraviolet (B-band) wave-lengths.[9] Pcs have been used in bulk heterojunction (BHJ) solar cells.[49,126,172,173] Some solar cell designs contain Zn(II) and Cu(II) Pc complexes and also contain various C_{60} derivatives, where vapour-deposition techniques are used to make specified layers.[126] Soluble dyes have also been used in layered devices or BHJ solar cells.[126,174] The commercially available fluorinated Pc platforms allow for click-type alkylation chemistry and the design of a series of robust, chemically compatible dyes with tuneable optical band gaps and energy levels.[42,48,49,126] The resulting dyes absorb a different portion of the solar spectrum in these devices. The semiconductor active layer is composed of a blend of Pc derivatives having different optical band gaps in order to capture a larger fraction of the solar spectrum. Substitution of peripheral fluoro groups on hexadecafluorophthalocyaninatozinc(II) ($ZnPcF_{16}$) by thioalkanes allows for better solubility. The frontier molecular orbitals (HOMO and LUMO) are primarily delocalized on the ring periphery. Substitution of electron-withdrawing groups with electron-donating groups outside the macrocycle affects the orbital energy levels.[126] The destabilization of the HOMO is more than the LUMO which results in decreased optical band gaps and the corresponding absorption wavelengths shift toward longer wavelengths in the NIR.[48,49,126] This substitution chemistry is used to cover a different and larger portion of the solar spectrum.

We have reported the substitution of thioalkyl substituents onto the $ZnPcF_{16}$ platform for fine-tuning the absorbance of this dye (Fig. 24).[126] The number of thioalkane *versus* fluorine substituents directly dictates the red-shift in the absorbance spectrum, especially of the Q-bands. There is a *ca*. 6.5 nm red shift for every fluorine substituted by thioalkane. Furthermore, solar cells made of blends of three dyes result in better efficiency than expected from individual dye performance because of broader coverage of the solar spectrum and synergistic charge migration. We also reported[49] on substituting the core $ZnPcF_{16}$ platform with diverse thioalkanes to control the morphology and the packing of dyes in BHJ devices (Fig. 24). Charge migration is not hindered because the Pc molecules have substantially overlapping HOMO–LUMO gaps. Similarly, from $ZnPcF_{16}$ we have synthesized[48] a dye bearing long alkane moieties on all 16 positions (Fig. 24). This promotes self-organization into nanoparticles and nano-films on indium tin oxide (ITO) and glass surfaces. The particles are highly mono-disperse and changing the concentration of the chromophores in solution can control their size upon surface deposition. We report the substitution of some thioalkyl groups but any primary thiolated moiety can be appended to investigate the role of exocyclic motifs in the properties of nanomaterials.

Por is also robust enough to be incorporated into light harvesting devices. Plants use various chlorophylls to cover as much of the solar spectrum as possible.[175] Natural dyes are not robust enough to be incorporated into devices because they are typically not stable for prolonged times, such as the span of years for a solar energy device. A useful solar cell would be expected to have 15–20 years of life. The $TPPF_{20}$ and PcF_{16} may be able to withstand these conditions, and so are considered to be good candidates for light harvesting. The maximum absorption of Por is a B (Soret) band at 390–430 nm with high molar coefficients and several Q-bands between 500 and 650 nm. Thus, $TPPF_{20}$ and its derivatives can be used to cover the blue end of the solar spectrum, while derivatives of PcF_{16} cover the red end. These macrocycles combined have good optical densities in the middle of the solar spectrum and afford a range of dyes to be incorporated into various devices.

We have done studies[42] using the $TPPF_{20}$ platform to put fluoroalkanes on the macrocycle to investigate the self-organization of the chromophore with C_{60} via a co-deposition process into thin-films (Fig. 25). We observed a significant quenching of the Por fluorescence because of electron transfer to the C_{60} electron acceptor. Král and co-workers[176] have also reported functionalizing the Por macrocycle with highly fluorous groups (Fig. 25). The authors suggest that the compounds have potential for drug delivery, transport of gases, and solar cells if mor-phological packing is appropriate.

For a PV device to work efficiently and properly there has to be a continuous conductive medium between the light absorbing dye and the electron acceptor to transfer the electron and create a charge separation. Our group has recently developed a Por dimer linked by a flexible dithiol tether (Fig. 26).[51] Upon mixing the dimer with C_{60} and C_{70} we discovered that it preferentially binds with fullerene C_{70} over C_{60} in toluene solution. The dimer–fullerene complex also forms stable aggregates when casted on glass. This type of binding study can open up opportunities for future research where the electron acceptor is kept in close proximity to the dye for a more efficient charge transfer without modification of the C_{60}, which is usually detrimental to the system.

We have shown[50,177] that click chemistry can be used to append thioalkyl tethers which can be attached to the Au surface for rapid assessment of chain length and dye association (Fig. 27). Free base and Zn(II) Por complexes were studied and both were found to bind near the edges of alkane thiol layer. Zn(II) complexes were observed to form small aggregates held together via π–π stacking or pyridyl–Zn interactions. Among these two the free base acts as a stochastic switch and the Zn(II) complex aggregates show evidence of a quantum cascade. The effective overlap of frontier orbitals favours charge transfer in the Zn(II) complex while minimal charge transfer was observed for the free base Por.

4. Conclusions and future perspectives

One major issue with the synthesis of functional groups co-valently bound to porphyrinoids for application in medicine and materials is the cost and ease of production at multigram scales. To bring the synthesis costs in the ranges for potential commercialization, straightforward and high yield synthetic organic strategies are needed for the construction of substituted porphyrinoid conjugates. Thus, the fluorinated porphyrinoids ($TPPF_{20}$, PcF_{16},

CF_{20}, IF_{20}, BF_{20} and $CorF_{15}$) are used as platforms to obtain an array of porphyrinoid derivatives *via* straightforward nucleophilic aromatic substitution. Compared to non-fluorinated porphyrinoid derivatives, fluorinated ones show an equally diverse range of physical and chemical properties. The presence of fluorines also improves the stability of these molecules to oxidative damage and brings further functionality. Various nucleophiles such as glycol, sugars, poly-amines, peptides, amino acids, and carboranes were substituted on fluorinated porphyrinoids in order to improve the biological efficacy, solar energy absorbance, molecular packing in thin films, catalytic activity and stability. Another advantage of this strategy is that various motifs such as disease targeting and for therapy can be readily tagged onto a fluorinated porphyrinoid. Lately, fused fluorinated porphyrinoids with NIR absorption and/or TPA have been investigated and showed potential as PS. These fluorinated porphyrinoid platforms continue to be exploited in designing drugs that can effectively target and treat diseases such as cancers, be the signal transducer in sensors, as catalysts, and to develop photonic films for solar cells. For the $ZnPcF_{16}$, exchange of the fluorine group for a thioalkane leads to a systematic red-shift of the absorbance spectrum, thereby creating a family of closely related dyes with substantial alignment of the HOMO–LUMO gaps, which then facilitate charge transport in materials composed of these dyes. Since the aryl groups on $TPPF_{20}$ are orthogonal to the macrocycle, substitution of the p-fluorine has only small effects on the photophysics. The ability to chelate to most metals allows for the creation of molecular catalysts and sensors.

Many biomolecules are robust under the conditions used for the nucleophilic substitution on these porphyrinoids, but some proteins and peptides may not. To append sensitive bio-molecules, *e.g.* antibodies, a tether can be appended on to the preformed fluorous porphyrinoid followed by conjugation of the sensitive biomolecule. The remaining fluorine groups present on these porphyrinoids after substitution (16 remaining on the $TPPF_{20}$, CF_{20}, IF_{20}, BF_{20} platforms; 12 remaining on the $CorF_{20}$ platform; and 1–15 remaining on the PcF_{16} plat-form) can be used as adjunct imaging modalities, *e.g.* ^{19}F NMR imaging, carbon–fluorine spectroscopy (CFR), and fluoro-Raman spectroscopy (FRS). Fluorines can be substituted with radio isotopes such as ^{18}F ($t_{1/2}$ = 110 min),[178,123] I($t_{1/2}$ = 13.22 hours),[179] and ^{131}I ($t_{1/2}$ = 8 days)[180] via reactions of fluorinated porphyrinoids with K18F/Na131I/Na123I and crown ethers. The K^+ and Na^+ chelator, kryptofix, may allow F-18, I-123 and I-131 labelling at elevated temperatures. ^{18}F porphyrinoids can be used as PET imaging agents without altering the photo-physics for fluorescence imaging, and ^{123}I porphyrinoids as single photon emission computed tomography (SPECT) imaging agents. ^{131}I can be used as radiotherapy and an imaging agent to treat cancers effectively as an adjuvant to PDT. The biomedical applications of fluorinated porphyrinoids have been reviewed.[16]

Por molecules have a propensity to bind with electron acceptors such as C_{60} and C_{70}. This opens a new window of research for further development of these materials where the electron acceptor is trapped in the complex allowing for a better connection and charge transfer. These complexes may result in more efficient solar cells and devices. Various thio-alkane nucleophiles have been substituted onto these core platforms, wherein the alkanes dictate nanostructure morphologies.[52,181] The mechanism of nanoparticle (NP) formation, the size of the NPs, the stability, and the organization of the Pors in the NPs exquisitely depend on the exact structure of the Por and the methods for making the NPs[181]

Recent advances in porphyrin-based metal–organic-frame-work (MOF) materials for catalysts, gas storage, and sensors build upon earlier work on the self-assembly of porphyrins by metal ion coordination.[10,182,183] Clicking metal ion coordination groups to these core platforms may facilitate the discovery and development of new MOF and hierarchically structured porphyrinoid materials. Hierarchical structure is of paramount importance for photonic materials.[184] As illustrated by the work described herein, these six and other fluorous porphyrinoid platforms enable the rapid, facile discovery of new theranostic, sensor, and photonic materials without complex, multistep reactions and tedious purifications.

Acknowledgements

This work was supported by the National Science Foundation – United States (NSF) through CHE-0847997 and CHE-1213962 to C. M. D. The science infrastructure of Hunter College is supported by the NSF, the City University of New York and the National Institute on Minority Health and Health Disparities of the National Institutes of Health under award number G12MD007599.

Biographies

N. V. S. Dinesh K. Bhupathiraju N. V. S. Dinesh K. Bhupathiraju was born in India. He obtained his Master’s degree in physical organic chemistry (2008) from Osmania University, India. He obtained his Ph.D. in organic chemistry (2013) from Louisiana State University, USA under the guidance of Prof. Maria Graça H. Vicente. Presently, he works as a visiting lecturer in the Department of Chemistry and Biochemistry and as a Research Associate in the laboratory of Prof. Charles M. Drain, Hunter College, CUNY. His research projects involve theranostic nanomedicines for cancer and the development of new dyes for solar energy harvesting materials for coating on windows in urban applications.

Waqar Rizvi Waqar Rizvi was born in Sialkot, Pakistan and moved to the U.S.A. at the age of eleven. He obtained his Bachelor’s degrees in Biochemistry and Bioinformatics (2012) from Hunter College of The City University of New York (CUNY). He is currently pursuing his Ph.D. in nanotechnology and materials chemistry at the Graduate Center, CUNY under the supervision of Prof. Charles M. Drain. His research focuses on developing new supramolecular porphyrinoid based dyes for materials and medicinal applications such as solar energy harvesting, biosensors, catalysts, cancer imaging and therapeutics. He is currently an adjunct lecturer at Hunter College, CUNY and teaches at First Academy, Little Neck, NY.

James D. Batteas James D. Batteas is a Professor of Chemistry and Materials Science and Engineering at Texas A&M University. He earned a B.S. in Chemistry from the University of Texas at Austin in 1990 and a Ph.D. in Chemistry from the University of California at Berkeley in 1995. He is an expert in materials chemistry of surfaces and interfaces with research activities covering a broad range of fundamental surface and interfacial phenomena. These include investigations of charge transport in organic molecules on surfaces (measured by STM and modeled by density functional theory), nanoparticle catalysis, semiconducting nanomaterials, plasmonics, tribology, “smart” surfaces, and selforganizing nanoscale materials for device applications in optoelectronics and chemical sensing. His research in tribology includes AFM studies of atomic scale friction and wear of oxides and 2D materials such as graphene. His group also employs the use of large-scale molecular dynamics simulations to explore the assemblies of molecules on nanoparticles and their interactions. He is a Fellow of the Royal Society of Chemistry and on the Editorial Boards of ACS Central Science and RSC Advances.

Charles Michael Drain Charles Michael Drain is Professor and Chair of Chemistry at Hunter College, CUNY and adjunct faculty at Rockefeller University. He started his career in chemistry at the University of Missouri in St. Louis. He received his Ph.D. from Tufts University in the laboratory of Barry B. Corden where he worked on porphyrin synthesis. He did postdoctoral work in the laboratory of David Mauzerall at Rockefeller University where he examined self-organizing systems composed of porphyrins and lipid bilayers and developed one of the first examples of a purely organic, synthetic phototransistor. He also examined all-D-amino acid-containing channel-forming antibiotic peptides with R. Bruce Merrifield. He was a guest researcher in the laboratory of Jean-Marie Lehn at the University Louis Pasteur in Strasbourg, France, where he developed methodologies to self-assemble porphyrins. Hewas a research fellow in the Holt Holten/Kirmaier laboratory at Washington University studying the complex dynamics of nickel porphyrins. Since joining Hunter College, 1996, his research continues to focus on the design, synthesis, and characterization of self-assembled and self-organized photonic systems.

Notes and references

1. *in* The Porphyrin Handbook-Applications: Past, Present and Future, ed. Kadish K, Smith KM and Guilard R, Academic Press, New York, 2000, vol. 6.
2. Guldi DM, Chem. Soc. Rev, 2002, 31, 22–36. [PubMed: 12108980]

3. Stich MIJ, Fischer LH and Wolfbeis OS, Chem. Soc. Rev, 2010, 39, 3102–3114. [PubMed: 20571676]
4. Senge MO, Fazekas M, Notaras EGA, Blau WJ, Zawadzka M, Locos OB and NiMhuircheartaigh EM, Adv. Mater, 2007, 19, 2737–2774.
5. Drain CM, Russell KC and Lehn J-M, Chem. Commun, 1996, 337–338.
6. Walter MG, Rudine AB and Wamser CC, J. Porphyrins Phthalocyanines, 2010, 14, 759–792.
7. Che C-M, Lo VK-Y, Zhou C-Y and Huang J-S, Chem. Soc. Rev, 2011, 40, 1950–1975. [PubMed: 21387046]
8. Nia S, Gong X, Drain CM, Jurow M, Rizvi W and Qureshy M, J. Porphyrins Phthalocyanines, 2010, 14, 621– 629.
9. Radivojevic A Varotto C Farley and Drain CM, Energy Environ. Sci, 2010, 3, 1897–1909.
10. Drain CM, Varotto A and Radivojevic I, Chem. Rev, 2009, 109, 1630–1658. [PubMed: 19253946]
11. Davia K, King D, Hong Y and Swavey S, Inorg. Chem. Commun, 2008, 11, 584–586.
12. Ko Y-J, Yun K-J, Kang M-S, Park J, Lee K-T, Park SB and Shin J-H, Bioorg. Med. Chem. Lett, 2007, 17, 2789– 2794. [PubMed: 17383879]
13. Ismail FMD, J. Fluorine Chem, 2002, 118, 27–33.
14. O'Hagan D and Rzepa HS, Chem. Commun, 1997, 645– 652.
15. Seebach D, Angew. Chem., Int. Ed. Engl, 1990, 29, 1320– 1367.
16. Goslinski T and Piskorz J, J. Photochem. Photobiol., C, 2011, 12, 304–321.
17. Silva AMG, Tomé AC, Neves MGPMS, Silva AMS and Cavaleiro JAS, J. Org. Chem, 2005, 70, 2306–2314. [PubMed: 15760219]
18. Silva AMG, Tomé AC, Neves MGPMS, Silva AMS and Cavaleiro JAS, Chem. Commun, 1999, 1767–1768.
19. Silva AMG, Tomé AC, Neves MGPMS and Cavaleiro JAS, Tetrahedron Lett, 2000, 41, 3065–3068.
20. Partlow KC, Chen J, Brant JA, Neubauer AM, Meyerrose TE, Creer MH, Nolta JA, Caruthers SD, Lanza GM and Wickline SA, FASEB J, 2007, 21, 1647– 1654. [PubMed: 17284484]
21. Murugesan R English S, Reijnders K, Yamada K.-i., Cook JA, Mitchell JB, Subramanian S and Krishna MC, Magn. Reson. Med, 2002, 48, 523–529. [PubMed: 12210918]
22. Golf HRA, Reissig H-U and Wiehe A, Eur. J. Org. Chem, 2015, 2015, 1548–1568.
23. Allred AL, J. Inorg. Nucl. Chem, 1961, 17, 215–221.
24. Tang Q, Li H, Liu Y and Hu W, J. Am. Chem. Soc, 2006, 128, 14634–14639. [PubMed: 17090049]
25. Buchler JW, in The Porphyrins, ed. Dolphin D, Academic, New York, 1978, vol. 1, pp. 389–483.
26. Kadish KM, Han BC, Franzen MM and AraulloMcAdams C, J. Am. Chem. Soc, 1990, 112, 8364–8368.
27. Battioni P, Brigaud O, Desvaux H, Mansuy D and Traylor TG, Tetrahedron Lett, 1991, 32, 2893–2896.
28. Kalisch WW and Senge MO, Angew. Chem., Int. Ed, 1998, 110, 1156–1159.
29. Senge MO, Acc. Chem. Res, 2005, 38, 733–743. [PubMed: 16171316]
30. McClure JE, Baudouin L, Mansuy D and Marzilli LG, Biopolymers, 1997, 42, 203–217. [PubMed: 9234999]
31. Chen X, Hui L, Foster DA and Drain CM, Biochemistry, 2004, 43, 10918–10929. [PubMed: 15323552]
32. Shaw SJ, Elgie KJ, Edwards C and Boyle RW, Tetrahedron Lett, 1999, 40, 1595–1596.
33. Hirohara S, Nishida M, Sharyo K, Obata M, Ando T and Tanihara M, Bioorg. Med. Chem, 2010, 18, 1526–1535. [PubMed: 20097078]
34. Shaw SJ, Edwards C and Boyle RW, Tetrahedron Lett, 1999, 40, 7585–7586.
35. Tian Y, Shumway BR and Meldrum DR, Chem. Mater, 2010, 22, 2069–2078. [PubMed: 20352057]
36. Santos F. d. C., Cunha AC, de Souza MCBV, Tomé AC, Neves MGPMS, Ferreira VF and Cavaleiro JAS, Tetrahedron Lett, 2008, 49, 7268–7270.

37. McKeown NB, Hanif S, Msayib K, Tattershall CE and Budd PM, Chem. Commun, 2002, 2782–2783.
38. Figueira ACB, de Oliveira KT and Serra OA, Dyes Pigm, 2011, 91, 383–388.
39. Samaroo D, Vinodu M, Chen X and Drain CM, J. Comb. Chem, 2007, 9, 998–1011. [PubMed: 17877415]
40. Kvíčala J, Beneš M, Paleta O and Král V, J. Fluorine Chem, 2010, 131, 1327–1337.
41. Bhupathiraju NVSDK, Hu X, Zhou Z, Fronczek FR, Couraud P-O, Romero IA, Weksler B and Vicente MGH, J. Med. Chem, 2014, 57, 6718–6728. [PubMed: 25029034]
42. Varotto A, Todaro L, Vinodu M, Koehne J, Liu G.-y. and Drain CM, Chem. Commun, 2008, 4921–4923.
43. Drain CM and Singh S, in The Handbook of Porphyrin Science with Applications to Chemistry, Physics, Materials Science, Engineering, Biology and Medicine, ed. Kadish K, Smith KM and Guilard R, World Scientific Publisher, Singapore, 2010, vol. 3, pp. 485–537.
44. Mironov AF and Grin MA, J. Porphyrins Phthalo-cyanines, 2008, 12, 1163–1172.
45. Králová J, Bříza T, Moserová I, Dolenský B, Vašek P, Poučková P, Kejík Z, Kaplánek R, Martásek P, Dvořák M and Král V, J. Med. Chem, 2008, 51, 5964–5973. [PubMed: 18788727]
46. Bhupathiraju NVSDK and Vicente MGH, Bioorg. Med. Chem, 2013, 21, 485–495. [PubMed: 23219853]
47. Singh S, Aggarwal A, Bhupathiraju NVSDK, Newton B, Nafees A, Gao R and Drain CM, Tetrahedron Lett, 2014, 55, 6311–6314. [PubMed: 25395694]
48. Jurow M, Varotto A, Manichev V, Travlou NA, Giannakoudakis DA and Drain CM, RSC Adv, 2013, 3, 21360–21364.
49. Jurow MJ, Hageman BA, DiMasi E, Nam C-Y, Pabon C, Black CT and Drain CM, J. Mater. Chem. A, 2013, 1, 1557–1565.
50. Schuckman AE, Ewers BW, Yu LH, Tomé JPC, Pérez LM, Drain CM, Kushmerick JG and Batteas JD, J. Phys. Chem. C, 2015, 119, 13569–13579.
51. Jurow M, Farley C, Pabon C, Hageman B, Dolor A and Drain CM, Chem. Commun, 2012, 48, 4731–4733.
52. Aggarwal A, Singh S, Samson J and Drain CM, Macro-mol. Rapid Commun, 2012, 33, 1220–1226.
53. Aggarwal A, Singh S and Drain CM, J. Porphyrins Phthalocyanines, 2011, 15, 1258–1264.
54. Ethirajan M, Chen Y, Joshi P and Pandey RK, Chem. Soc. Rev, 2011, 40, 340–362. [PubMed: 20694259]
55. Dougherty TJ, Gomer CJ, Henderson BW, Jori G, Kessel D, Korbelik M, Moan J and Peng Q, J. Natl. Cancer Inst, 1998, 90, 889–905. [PubMed: 9637138]
56. Jichlinski P and Leisinger H-J, Urol. Res, 2001, 29, 396–405. [PubMed: 11828993]
57. Dolmans DEJGJ, Fukumura D and Jain RK, Nat. Rev. Cancer, 2003, 3, 380–387. [PubMed: 12724736]
58. Detty MR, Gibson SL and Wagner SJ, J. Med. Chem, 2004, 47, 3897–3915. [PubMed: 15267226]
59. Fritsch C, Goerz G and Ruzicka T, Arch. Dermatol, 1998, 134, 207–214. [PubMed: 9487213]
60. Szeimies R-M, Landthaler M and Karrer S, J. Dermatol. Treat, 2002, 13, s13–s18.
61. Bonneau S and Vever-Bizet C, Expert Opin. Ther. Pat, 2008, 18, 1011–1025.
62. Phillips D, Photochem. Photobiol. Sci, 2010, 9, 1589–1596. [PubMed: 21082123]
63. Konopka K and Goslinski T, J. Dent. Res, 2007, 86, 694–707. [PubMed: 17652195]
64. Kubin A, Wierrani F, Burner U, Alth G and Grunberger W, Curr. Pharm. Des, 2005, 11, 233–253. [PubMed: 15638760]
65. Trannoy LL, Lagerberg JWM, Dubbelman TMAR, Schuitmaker HJ and Brand A, Transfusion, 2004, 44, 1186–1196. [PubMed: 15265123]
66. Tomé JPC, Neves MGPMS, Tomé AC, Cavaleiro JAS, Soncin M, Magaraggia M, Ferro S and Jori G, J. Med. Chem, 2004, 47, 6649–6652. [PubMed: 15588101]
67. Singh S, Aggarwal A, Bhupathiraju NVSDK, Arianna G, Tiwari K and Drain CM, Chem. Rev, 2015, 115, 10261–10306. [PubMed: 26317756]

68. Hao E, Friso E, Miotto G, Jori G, Soncin M, Fabris C, Sibrian-Vazquez M and Vicente MGH, Org. Biomol. Chem, 2008, 6, 3732–3740. [PubMed: 18843403]
69. Hiramatsu R, Kawabata S, Tanaka H, Sakurai Y, Suzuki M, Ono K, Miyatake S-I, Kuroiwa T, Hao E and Vicente MGH, J. Pharm. Sci, 2015, 104, 962–970.
70. Belle C, Béguin C, Hamman S and Pierre J-L, Coord. Chem. Rev, 2009, 253, 963–976.
71. Malet-Martino M, Gilard V, Desmoulin F and Martino R, Clin. Chim. Acta, 2006, 366, 61–73. [PubMed: 16337167]
72. Martino R, Gilard V, Desmoulin F and Malet-Martino M, J. Pharm. Biomed. Anal, 2005, 38, 871–891. [PubMed: 16087049]
73. Couturier O, Luxen A, Chatal J-F, Vuillez J-P, Rigo P and Hustinx R, Eur. J. Nucl. Med. Mol. Imaging, 2004, 31, 1182–1206. [PubMed: 15241631]
74. Menaa F, Menaa B and Sharts O, Faraday Discuss, 2011, 149, 269–278. [PubMed: 21413185]
75. Ahmed S, Davoust E, Savoie H, Boa AN and Boyle RW, Tetrahedron Lett, 2004, 45, 6045–6047.
76. Pasetto P, Chen X, Drain CM and Franck RW, Chem. Commun, 2001, 81–82.
77. Hirohara S, Obata M, Alitomo H, Sharyo K, Ando T, Yano S and Tanihara M, Bioconjugate Chem, 2009, 20, 944–952.
78. Tomé JPC, Neves MGPMS, Tomé AC, Cavaleiro JAS, Mendonça AF, Pegado IN, Duarte R and Valdeira ML, Bioorg. Med. Chem, 2005, 13, 3878– 3888. [PubMed: 15911304]
79. Samaroo D, Soll CE, Todaro LJ and Drain CM, Org. Lett, 2006, 8, 4985–4988. [PubMed: 17048824]
80. Mewis RE, Savoie H, Archibald SJ and Boyle RW, Photodiagn. Photodyn. Ther, 2009, 6, 200–206.
81. Serra VV, Camoes F, Vieira SI, Faustino MAF, Tomé JPC, Pinto DCGA, Neves MGPMS, Tomé AC, Silva AMS, da Cruz e Silva EF and Cavaleiro JAS, Acta Chim. Slov, 2009, 56, 603–611.
82. Králová J, Kejík Z, Bříza T, Poučková P, Král A, Martásek P and Král V, J. Med. Chem, 2010, 53, 128– 138. [PubMed: 19950899]
83. Pedrosa LF, de Souza MC, Faustino MAF, Neves MGPMS, Silva AMS, Tomé AC, Ferreira VF and Cavaleiro JAS, Aust. J. Chem, 2011, 64, 939–944.
84. Gomes MC, Woranovicz-Barreira SM, Faustino MAF, Fernandes R, Neves MGPMS, Tomé AC, Gomes NCM, Almeida A, Cavaleiro JAS, Cunha A and Tomé JPC, Photochem. Photobiol. Sci, 2011, 10, 1735–1743. [PubMed: 21858350]
85. Costa DCS, Pais VF, Silva AMS, Cavaleiro JAS, Pischel U and Tomé JPC, Tetrahedron Lett, 2014, 55, 4156–4159.
86. Sternberg ED, Dolphin D and Brückner C, Tetrahedron, 1998, 54, 4151–4202.
87. Bonnett R, Chem. Soc. Rev, 1995, 24, 19–33.
88. Pandey RK, J. Porphyrins Phthalocyanines, 2000, 4, 368– 373.
89. Olshevskaya V, Zaitsev AV, Sigan AL, Kononova EG, Petrovskii PV, Chkanikov ND and Kalinin VN, Dokl. Chem, 2010, 435, 334–338.
90. Drain CM, Singh S, Samaroo D, Thompson S, Vinodu M and Tomé JPC, Proc. SPIE, 2009, 7380, 73902K.
91. Hirohara S, Obata M, Alitomo H, Sharyo K, Ando T, Tanihara M and Yano S, J. Photochem. Photobiol., B, 2009, 97, 22–33. [PubMed: 19679489]
92. Singh S, Aggarwal A, Thompson S, Tomé JPC, Zhu X, Samaroo D, Vinodu M, Gao R and Drain CM, Bio-conjugate Chem, 2010, 21, 2136–2146.
93. Aggarwal A, Thompson S, Singh S, Newton B, Moore A, Gao R, Gu X, Mukherjee S and Drain CM, Photochem. Photobiol, 2014, 90, 419–430. [PubMed: 24112086]
94. Hirohara S, Kawasaki Y, Funasako R, Yasui N, Totani M, Alitomo H, Yuasa J, Kawai T, Oka C, Kawaichi M, Obata M and Tanihara M, Bioconjugate Chem, 2012, 23, 1881–1890.
95. Azenha EG, Serra AC, Pineiro M, Pereira MM, Seixas de Melo J, Arnaut LG, Formosinho SJ and Rocha Gonsalves A. M. d. A., Chem. Phys, 2002, 280, 177– 190.
96. Gorman A, Killoran J, O'Shea C, Kenna T, Gallagher WM and O'Shea DF, J. Am. Chem. Soc, 2004, 126, 10619–10631. [PubMed: 15327320]

97. Sakuma S, Otake E, Torii K, Nakamura M, Maeda A, Tujii R, Akashi H, Ohi H, Yano S and Morita A, J. Porphyrins Phthalocyanines, 2013, 17, 331–342.

98. Tanaka M, Kataoka H, Mabuchi M, Sakuma S, Takahashi S, Tujii R, Akashi H, Ohi H, Yano S, Morita A and Joh T, Anticancer Res, 2011, 31, 763–770. [PubMed: 21498693]

99. Ogikubo J, Worlinsky JL, Fu Y-J and Brückner C, Tetra-hedron Lett, 2013, 54, 1707–1710.

100. Gross Z, Galili N and Saltsman I, Angew. Chem., Int. Ed, 1999, 38, 1427–1429.

101. Ventura B, Degli Esposti A, Koszarna B, Gryko DT and Flamigni L, New J. Chem, 2005, 29, 1559–1566.

102. Lili Y, Han S, Lei S, GuoLiang Z, HaiYang L, Hui W and LiangNian J, Sci. China: Phys., Mech. Astron, 2010, 53, 1491–1496

103. Gryko DT and Koszarna B, Org. Biomol. Chem, 2003, 1, 350–357. [PubMed: 12929430]

104. Gross Z and Galili N, Angew. Chem., Int. Ed, 1999, 38, 2366–2369.

105. Cardote TAF, Barata JFB, Faustino MAF, Preuß A, Neves MGPMS, Cavaleiro JAS, Ramos CIV, Santana-Marques MGO and Röder B, Tetrahedron Lett, 2012, 53, 6388–6393.

106. Hori T and Osuka A, Eur. J. Org. Chem, 2010, 2010, 2379–2386.

107. Schmidlehner M, Faschinger F, Reith LM, Ertl M and Schoefberger W, Appl. Organomet. Chem, 2013, 27, 395– 405.

108. Lourenc LMO, Neves MGPMS, Cavaleiro JAS and Tomé JPC, Tetrahedron, 2014, 70, 2681–2698.

109. Roeder B, Naether D, Lewald T, Braune M, Nowak C and Freyer W, Biophys. Chem, 1990, 35, 303–312. [PubMed: 2397276]

110. Sekkat N, Bergh H. v. d., Nyokong T and Lange N, Molecules, 2011, 17, 98–144. [PubMed: 22198535]

111. Phthalocyanines, Properties and Applications, ed. Leznoff CC and Lever ABP, Wiley VCH, New York, 1989.

112. Aggarwal A, Singh S, Zhang Y, Anthes M, Samaroo D, Gao R and Drain CM, Tetrahedron Lett, 2011, 52, 5456– 5459. [PubMed: 21966031]

113. Silva S, Pereira PMR, Silva P, Almeida Paz FA, Faustino MAF, Cavaleiro JAS and Tomé JPC, Chem. Commun, 2012, 48, 3608–3610.

114. Pereira PM, Silva S, Cavaleiro JA, Ribeiro CA, Tomé JP and Fernandes R, PLoS One, 2014, 9, e95529– e95541. [PubMed: 24763311]

115. Pereira JB, Carvalho EFA, Faustino MAF, Fernandes R, Neves MGPMS, Cavaleiro JAS, Gomes NCM, Cunha A, Almeida A and Tomé JPC, Photochem. Photobiol, 2012, 88, 537–547. [PubMed: 22332603]

116. Lourenco LMO, Pereira PMR, Maciel E, Valega M, Domingues FMJ, Domingues MRM, Neves MGPMS, Cavaleiro JAS, Fernandes R and Tomé JPC, Chem. Commun, 2014, 50, 8363–8366.

117. Singh S, Aggarwal A, Thompson S, Tomé JPC, Zhu X, Samaroo D, Vinodu M, Gao R and Drain CM, Bio-conjugate Chem, 2010, 21, 2136–2146.

118. Achelle S, Couleaud P, Baldeck P, Teulade-Fichou M-P and Maillard P, Eur. J. Org. Chem, 2011, 1271– 1279.

119. Mori H, Tanaka T, Aratani N, Lee BS, Kim P, Kim D and Osuka A, Chem. – Asian J, 2012, 7, 1811–1816. [PubMed: 22615269]

120. Castro KADF, Silva S, Pereira PMR, Simões MMQ, Neves M. d. G. P. M. S., Cavaleiro JAS, Wypych F, Tomé JPC and Nakagaki S, Inorg. Chem, 2015, 54, 4382–4393. [PubMed: 25897563]

121. Castro KADF, Simoes MMQ, Neves MGPMS, Cavaleiro JAS, Wypych F and Nakagaki S, Catal. Sci. Technol, 2014, 4, 129–141.

122. Hall JFB, Han X, Poliakoff M, Bourne RA and George MW, Chem. Commun, 2012, 48, 3073–3075.

123. Lipińska ME, Rebelo SLH and Freire C, J. Mater. Sci, 2014, 49, 1494–1505.

124. Mackintosh HJ, Budd PM and McKeown NB, J. Mater. Chem, 2008, 18, 573–578.

125. Yang J, Gabriele B, Belvedere S, Huang Y and Breslow R, J. Org. Chem, 2002, 67, 5057–5067. [PubMed: 12126389]

126. Varotto A, Nam C-Y, Radivojevic I, Tomé JPC, Cavaleiro JAS, Black CT and Drain CM, J. Am. Chem. Soc, 2010, 132, 2552–2554. [PubMed: 20136126]
127. Rutishauser J and Kopp P, Eur. J. Endocrinol, 1998, 138, 623–624. [PubMed: 9678527]
128. Carvalho de Medeiros MA, Gorgy K, Deronzier A and Cosnier S, Mater. Sci. Eng., C, 2008, 28, 731–738.
129. Liu SF, Petty AR, Sazama GT and Swager TM, Angew. Chem., Int. Ed, 2015, 54, 6554–6557.
130. Worlinsky JL, Halepas S and Bruckner C, Org. Biomol. Chem, 2014, 12, 3991–4001. [PubMed: 24825173]
131. Yella A, Lee H-W, Tsao HN, Yi C, Chandiran AK, Nazeeruddin MK, Diau EW-G, Yeh C-Y, Zakeeruddin SM and Grätzel M, Science, 2011, 334, 629–634. [PubMed: 22053043]
132. Batabyal D, Li H and Poulos TL, Biochemistry, 2013, 52, 5396–5402. [PubMed: 23865948]
133. Smeureanu G, Aggarwal A, Soll CE, Arijeloye J, Malave E and Drain CM, Chemistry, 2009, 15, 12133– 12140. [PubMed: 19777510]
134. Eckshtain M, Zilbermann I, Mahammed A, Saltsman I, Okun Z, Maimon E, Cohen H, Meyerstein D and Gross Z, Dalton Trans, 2009, 7879–7882. [PubMed: 19771348]
135. Kudrik EV, Afanasiev P, Alvarez LX, Dubourdeaux P, Clémancey M, Latour J-M, Blondin G, Bouchu D, Albrieux F, Nefedov SE and Sorokin AB, Nat. Chem, 2012, 4, 1024–1029. [PubMed: 23174983]
136. Liu Q and Guo CC, Sci. China: Chem, 2012, 55, 2036– 2053.
137. Salvador JAR, Moreira VM, Pinto RMA, Leal AS and Paixão JA, Beilstein J. Org. Chem, 2012, 8, 164– 169. [PubMed: 22423283]
138. Ellis PE, Jr., Lyons JE and Shaikh SN, Catal. Lett, 1994, 24, 79–83.
139. Costa L, Faustino MAF, Neves MGPMS, Cunha Â and Almeida A, Viruses, 2012, 4, 1034–1074. [PubMed: 22852040]
140. Zanoni TB, Lizier TM, Assis M. d. D., Zanoni MVB and de Oliveira DP, Food Chem. Toxicol, 2013, 57, 217– 226. [PubMed: 23562707]
141. Simões MMQ, De Paula R, Neves MGPMS and Cavaleiro JAS, J. Porphyrins Phthalocyanines, 2009, 13, 589–596.
142. Shen D.-h., Ji L.-t., Fu L.-l., Dong X.-l., Liu Z.-g., Liu Q and Liu S.-m., J. Cent. South Univ, 2015, 22, 862–867.
143. Machado GS, Groszewicz PB, Castro K. A. D. d. F., Wypych F and Nakagaki S, J. Colloid Interface Sci, 2012, 374, 278–286. [PubMed: 22402183]
144. Kato R, Kobayashi Y, Akiyama M and Komatsu T, Dalton Trans, 2013, 42, 15889–15892. [PubMed: 23842868]
145. Li L and Hu G.-k., Biosci. Rep, 2015, 35, e00174. [PubMed: 25608948]
146. Batinic-Haberle I, Spasojevic I, Stevens RD, Hambright P, Neta P, Okado-Matsumoto A and Fridovich I, Dalton Trans, 2004, 1696–1702. [PubMed: 15252564]
147. Durr K, Macpherson BP, Warratz R, Hampel F, Tuczek F, Helmreich M, Jux N and Ivanovic-Burmazovic I, J. Am. Chem. Soc, 2007, 129, 4217–4228 [PubMed: 17371019]
148. Gale PA, Acc. Chem. Res, 2011, 44, 216–226. [PubMed: 21207951]
149. Hoffmann EK, Biochim. Biophys. Acta, 1986, 864, 1–31. [PubMed: 3521744]
150. Rutishauser J and Kopp P, Eur. J. Endocrinol, 1998, 138, 623–624. [PubMed: 9678527]
151. Beer PD and Gale PA, Angew. Chem., Int. Ed, 2001, 40, 486–516.
152. Rodrigues JMM, Farinha ASF, Muteto PV, Woranovicz-Barreira SM, Almeida Paz FA, Neves MGPMS, Cavaleiro JAS, Tomé AC, Gomes MTSR, Sessler JL and Tomé JPC, Chem. Commun, 2014, 50, 1359–1361.
153. Prados P and Quesada R, Supramol. Chem, 2008, 20, 201–216.
154. Kubik S, Reyheller C and Stüwe S, J. Inclusion Phenom. Macrocyclic Chem, 2005, 52, 137–187.
155. Verdejo B, Rodriguez-Llansola F, Escuder B, Miravet JF and Ballester P, Chem. Commun, 2011, 47, 2017–2019.
156. Palomares E, Martínez-Díaz MV, Torres T and Coronado E, Adv. Funct. Mater, 2006, 16, 1166–1170.

157. Santos CIM, Oliveira E, Barata JFB, Faustino MAF, Cavaleiro JAS, Neves MGPMS and Lodeiro C, J. Mater. Chem, 2012, 22, 13811–13819.
158. Cormode DP, Drew MGB, Jagessar R and Beer PD, Dalton Trans, 2008, 6732–6741, DOI: 10.1039/B807153E. [PubMed: 19153621]
159. Amao Y, Microchim. Acta, 2003, 143, 1–12.
160. Wang X.-d., Chen X, Xie Z.-x. and Wang X.-r., Angew. Chem., Int. Ed, 2008, 47, 7450–7453.
161. Hasumoto H, Imazu T, Miura T and Kogure K, J. Oceanogr, 2006, 62, 99–103.
162. Tian Y, Shumway BR, Gao W, Youngbull C, Holl MR, Johnson RH and Meldrum DR, Sens. Actuators, B, 2010, 150, 579–587.
163. Stich MIJ, Schaeferling M and Wolfbeis OS, Adv. Mater, 2009, 21, 2216–2220.
164. Nagl S and Wolfbeis OS, Analyst, 2007, 132, 507–511. [PubMed: 17525805]
165. Borisov SM, Vasylevska AS, Krause C and Wolfbeis OS, Adv. Funct. Mater, 2006, 16, 1536–1542.
166. Köse ME, Carroll BF and Schanze KS, Langmuir, 2005, 21, 9121–9129. [PubMed: 16171341]
167. Han B-H, Manners I and Winnik MA, Anal. Chem, 2005, 77, 8075–8085. [PubMed: 16351158]
168. Lee S-K and Okura I, Anal. Commun, 1997, 34, 185–188.
169. Friswell MR, European patent no 0509818A1, 1992.
170. Krutak JJ, Cushaman MR and Waever MA, US patent no 5525516, 1996.
171. Puangmalee S, Petsom A and Thamyongkit P, Dyes Pigm, 2009, 82, 26–30.
172. de la Torre G, Claessens CG and Torres T, Chem. Commun, 2007, 2000–2015.
173. Honda S, Nogami T, Ohkita H, Benten H and Ito S, ACS Appl. Mater. Interfaces, 2009, 1, 804–810. [PubMed: 20356005]
174. Walker B, Tamayo AB, Dang X-D, Zalar P, Seo JH, Garcia A, Tantiwiwat M and Nguyen T-Q, Adv. Funct. Mater, 2009, 19, 3063–3069.
175. Calogero G, Di Marco G, Cazzanti S, Caramori S, Argazzi R, Di Carlo A and Bignozzi CA, Int. J. Mol. Sci, 2010, 11, 254–267. [PubMed: 20162014]
176. Bříza T, Kaplánek R, Havlík M, Dolenský B, Kejík Z, Martásek P and Král V, Supramol. Chem, 2008, 20, 237– 242.
177. Chan Y-H, Schuckman AE, Pérez LM, Vinodu M, Drain CM and Batteas JD, J. Phys. Chem. C, 2008, 112, 6110–6118.
178. Jacobson O, Kiesewetter DO and Chen X, Bioconjugate Chem, 2015, 26, 1–18.
179. Jacquemin R, Int. J. Radiat. Appl. Instrum., Part A, 1987, 38, 1087–1089.
180. Rose PS, Smith JP, Aller RC, Cochran JK, Swanson RL and Coffin RB, Environ. Sci. Technol, 2015, 49, 10312–10319. [PubMed: 26008140]
181. Drain CM, Smeureanu G, Patel S, Gong X, Garno J and Arijeloye J, New J. Chem, 2006, 30, 1834–1843.
182. Drain CM, Nifiatis F, Vasenko A and Batteas JD, Angew. Chem., Int. Ed, 1998, 37, 2344–2347.
183. Drain CM and Lehn J-M, J. Chem. Soc., Chem. Commun, 1994, 2313–2315, DOI: 10.1039/C39940002313.
184. Jurow MJ, Mayr C, Schmidt TD, Lampe T, Djurovich PI, Brutting W and Thompson ME, Nat. Mater, 2015, advance online publication.

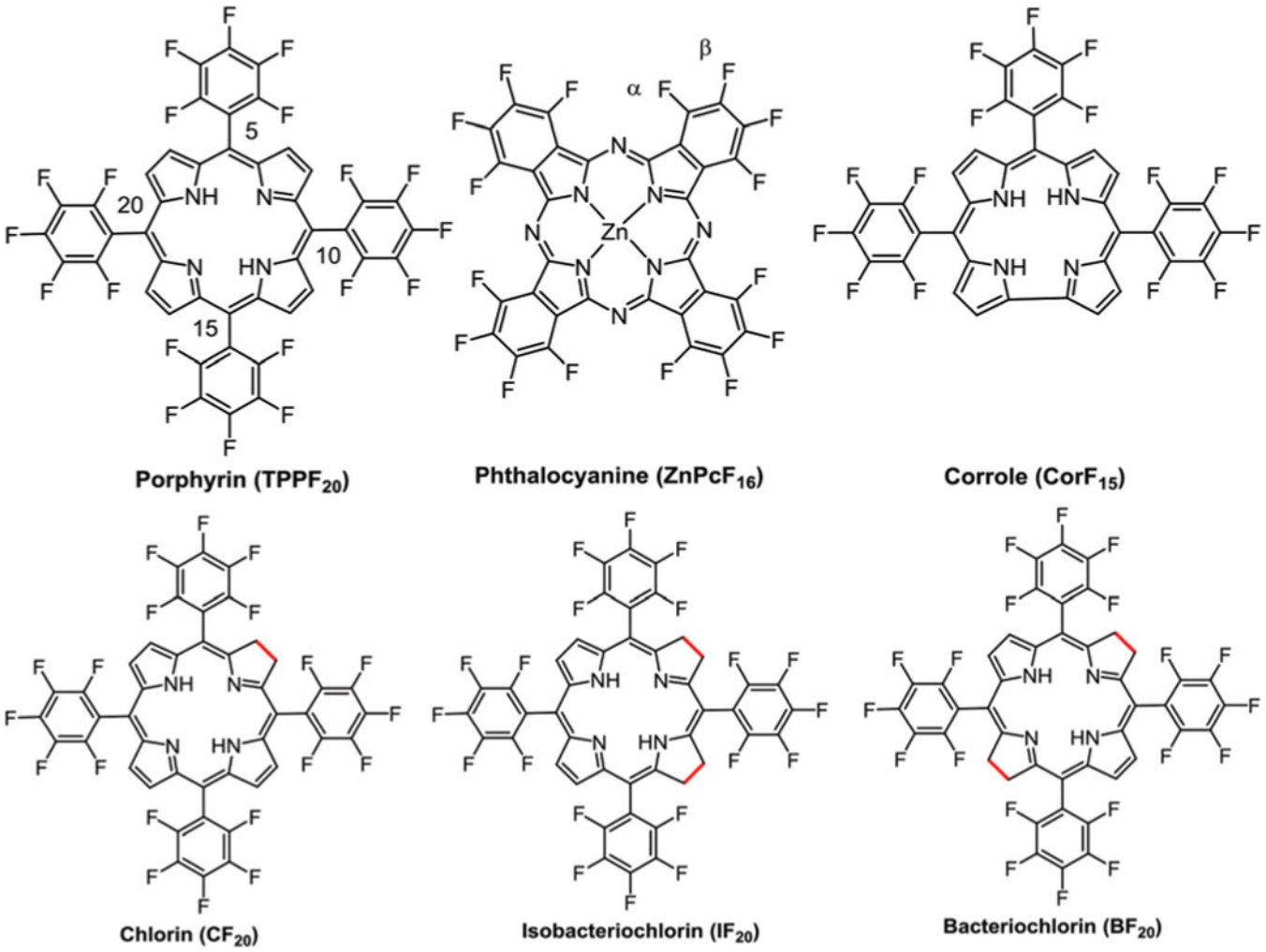

Fig. 1.
Fluorinated porphyrinoid platforms.

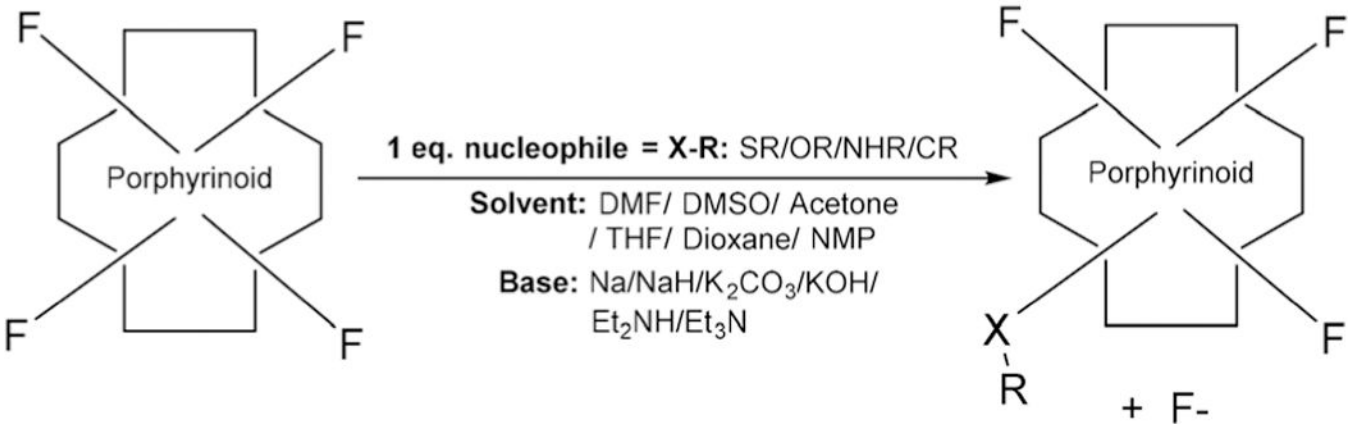

Fig. 2.

Scheme of nucleophilic substitution on fluorinated porphyrinoids (substitution in the order of softness: S > N > O).

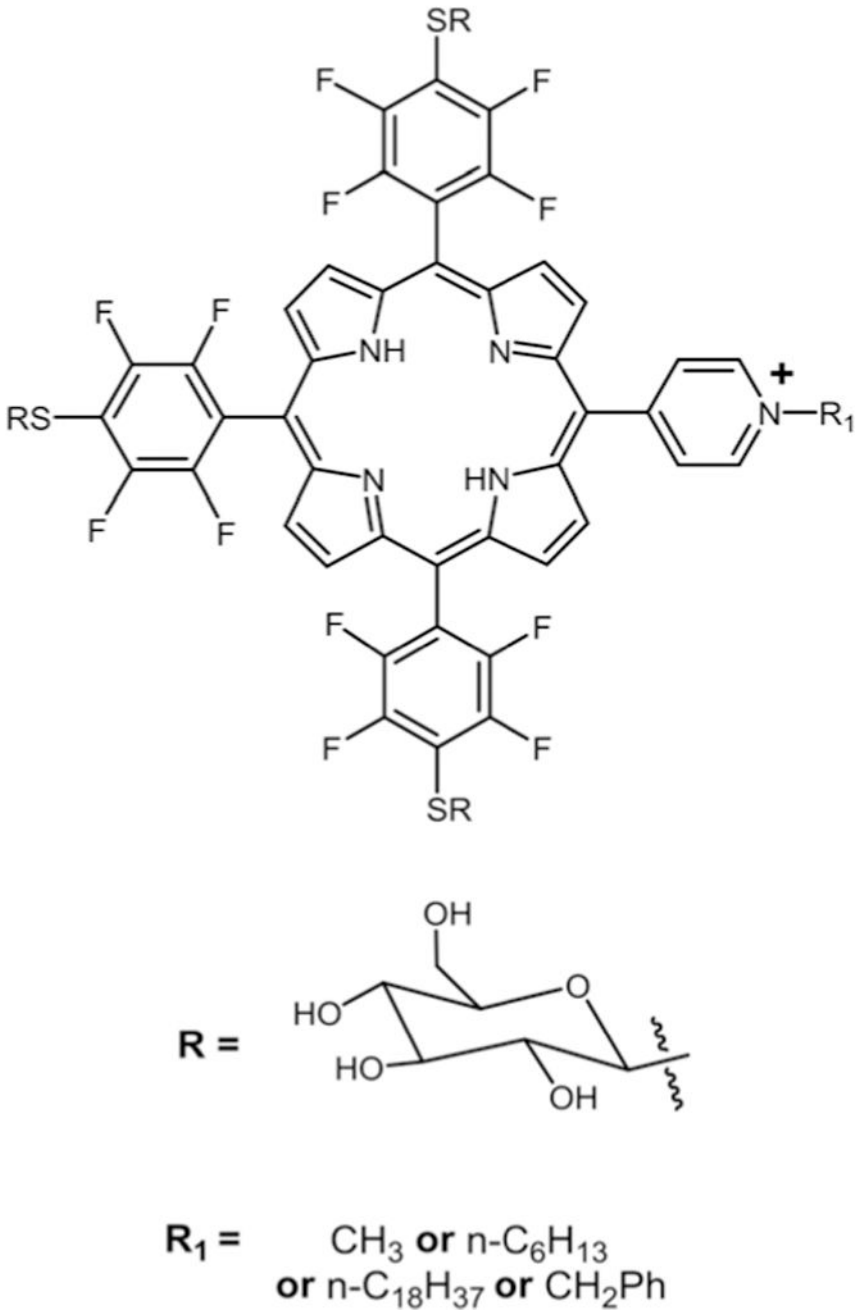

Fig. 3.
Thioglycosylated cationic porphyrin, see ref. 75.

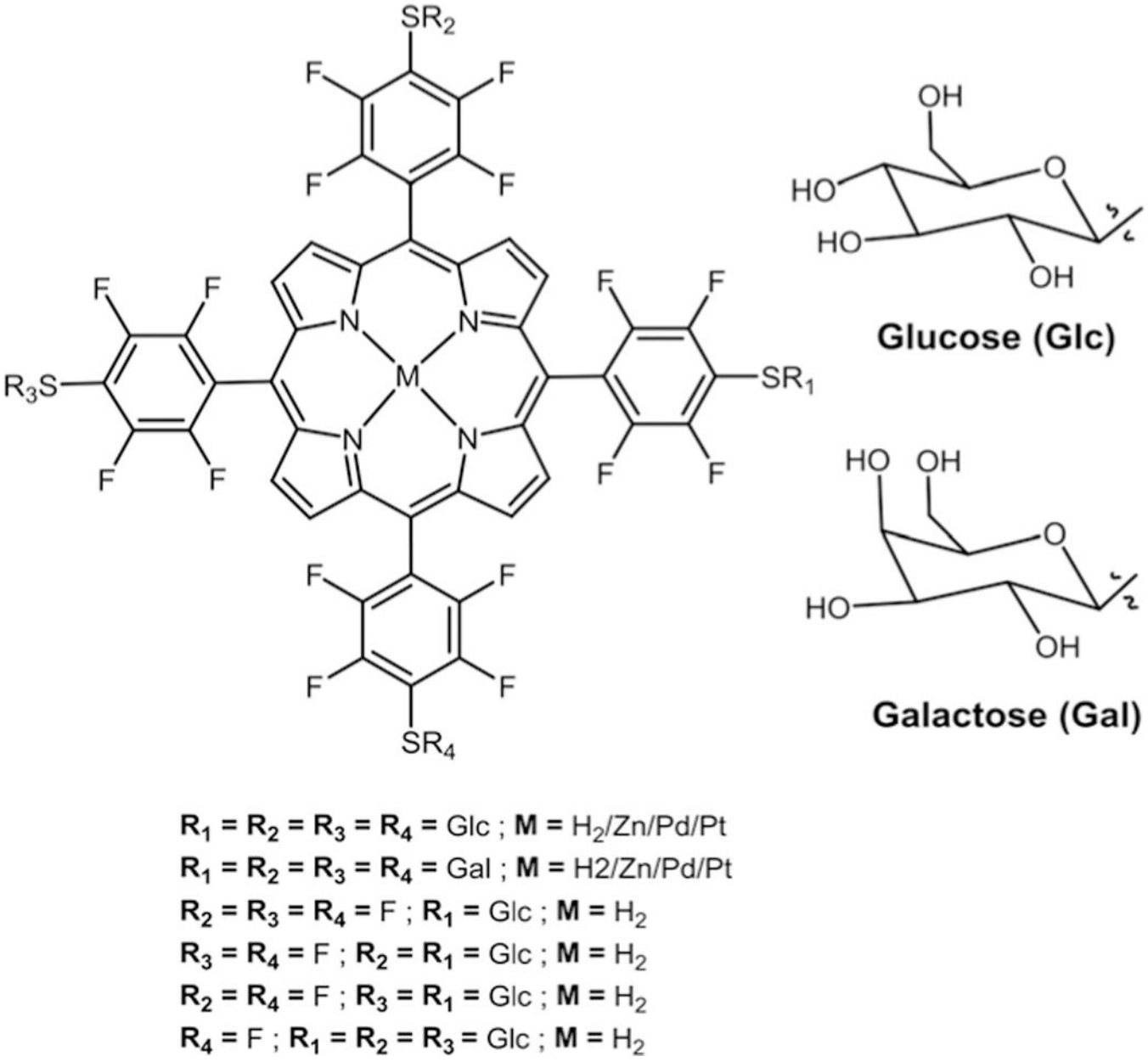

R_1 = R_2 = R_3 = R_4 = Glc ; **M** = H_2/Zn/Pd/Pt
R_1 = R_2 = R_3 = R_4 = Gal ; **M** = H2/Zn/Pd/Pt
R_2 = R_3 = R_4 = F ; **R_1** = Glc ; **M** = H_2
R_3 = R_4 = F ; **R_2 = R_1** = Glc ; **M** = H_2
R_2 = R_4 = F ; **R_3 = R_1** = Glc ; **M** = H_2
R_4 = F ; **R_1 = R_2 = R_3** = Glc ; **M** = H_2

Fig. 4.
Metallated and non-metallated S-sugar-porphyrins, see ref. 33, 76, and 77.

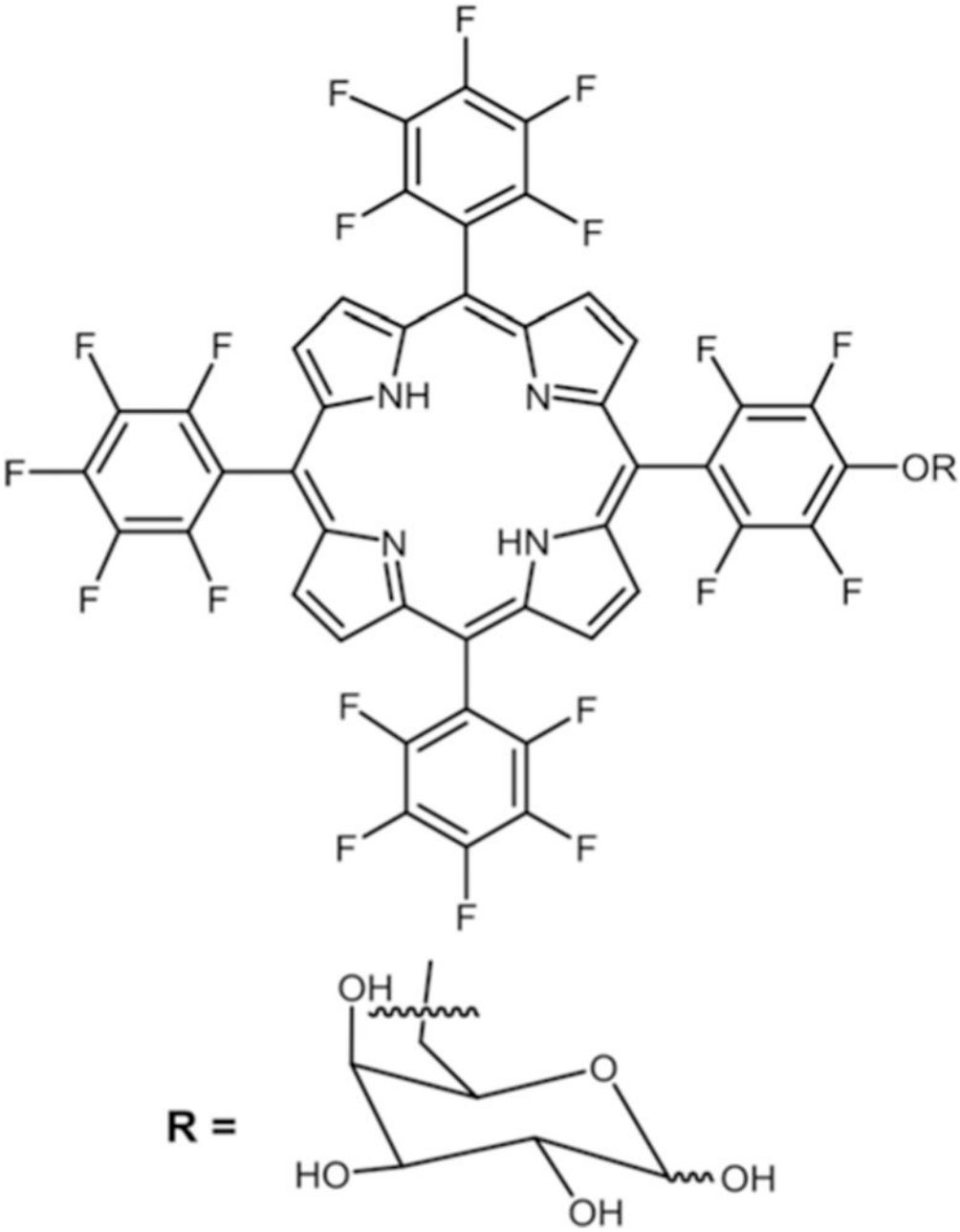

Fig. 5.
Mono substituted O-galactosyl porphyrin, see ref. 78.

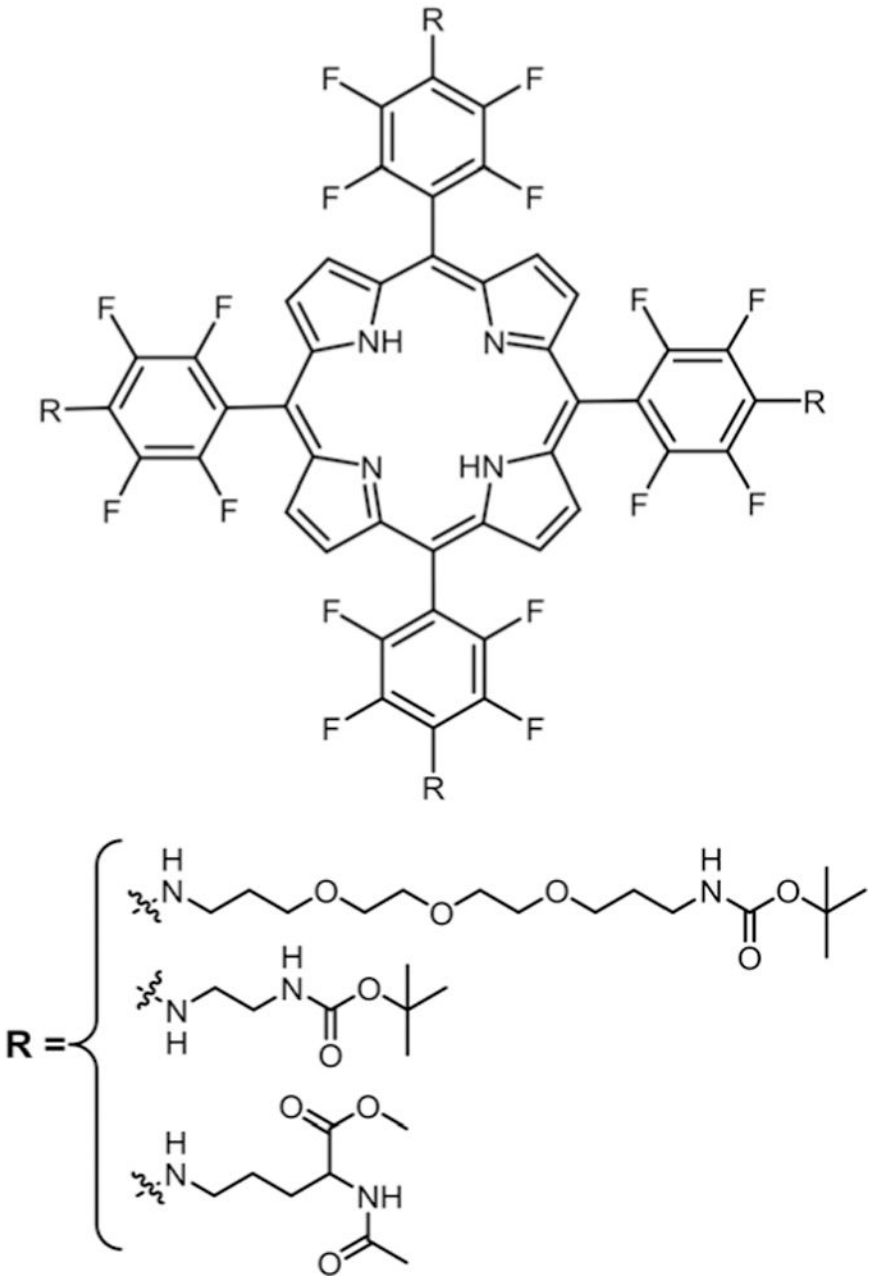

Fig. 6.
Symmetric tetra amino substituted porphyrin, see ref. 79.

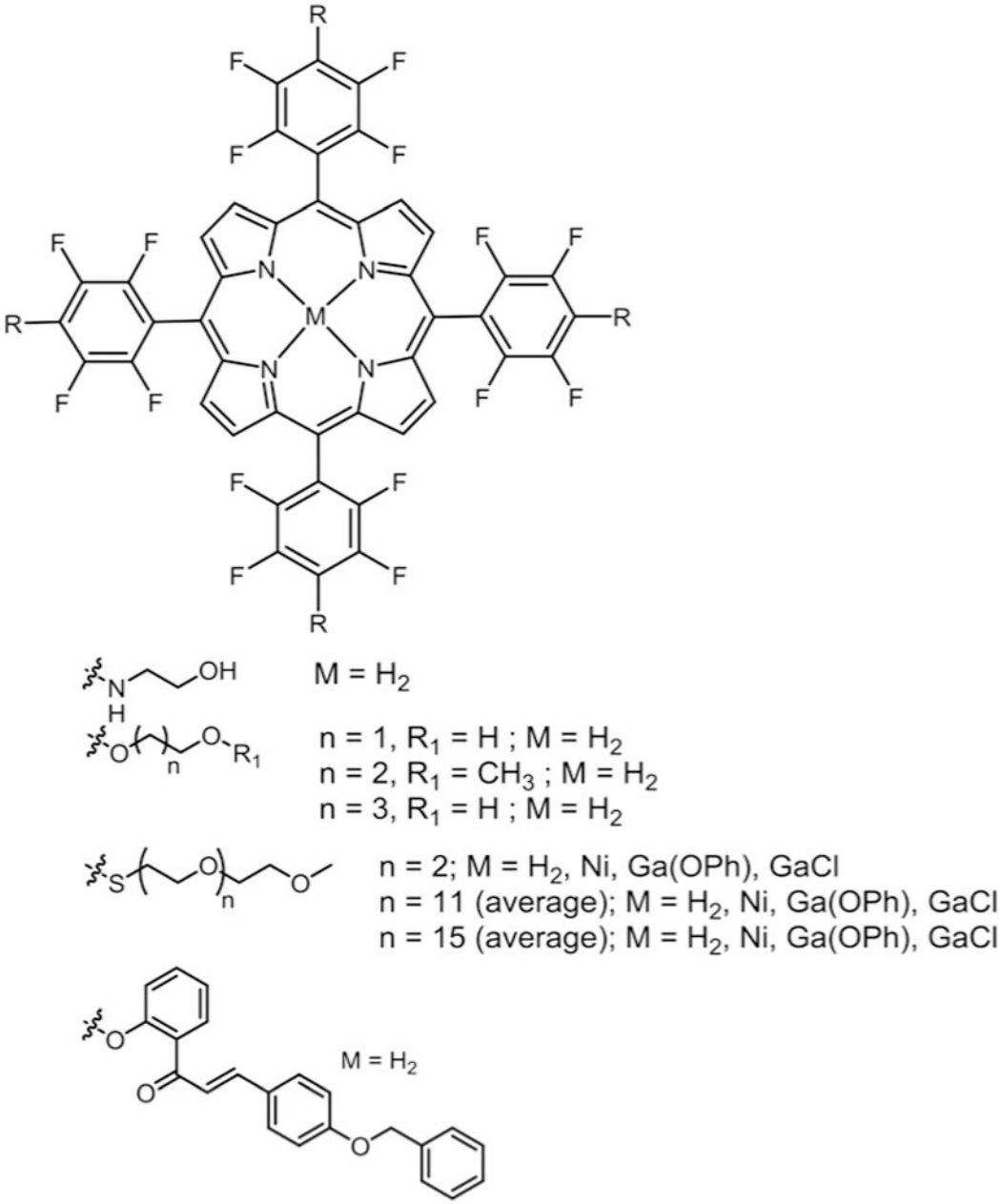

Fig. 7.

Symmetric metallated and metal free glycol porphyrins and free base chalcone porphyrin derivatives, see ref. 45, 80, and 81.

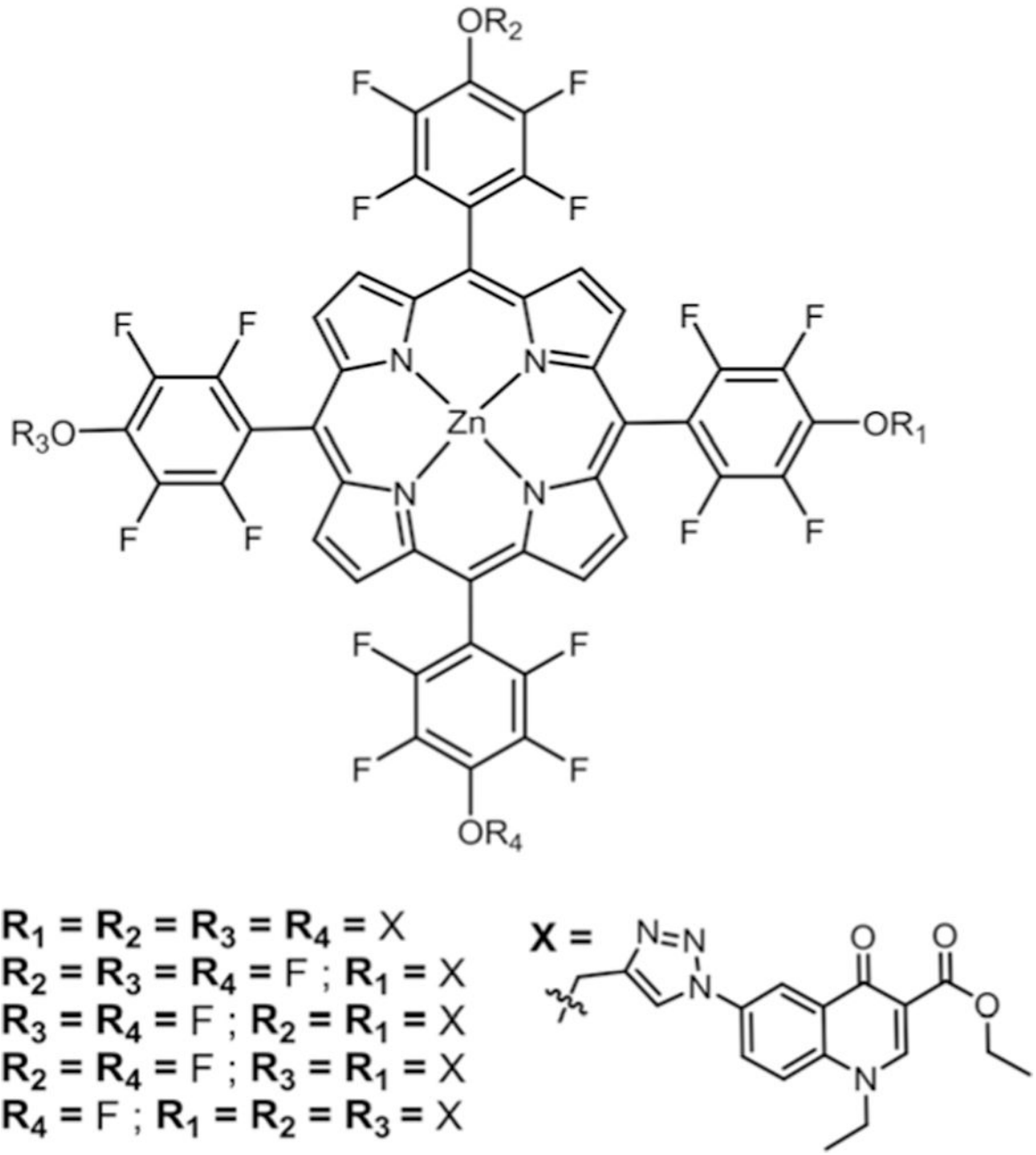

Fig. 8.
Zinc metallated porphyrin–quinolone conjugates, see ref. 36.

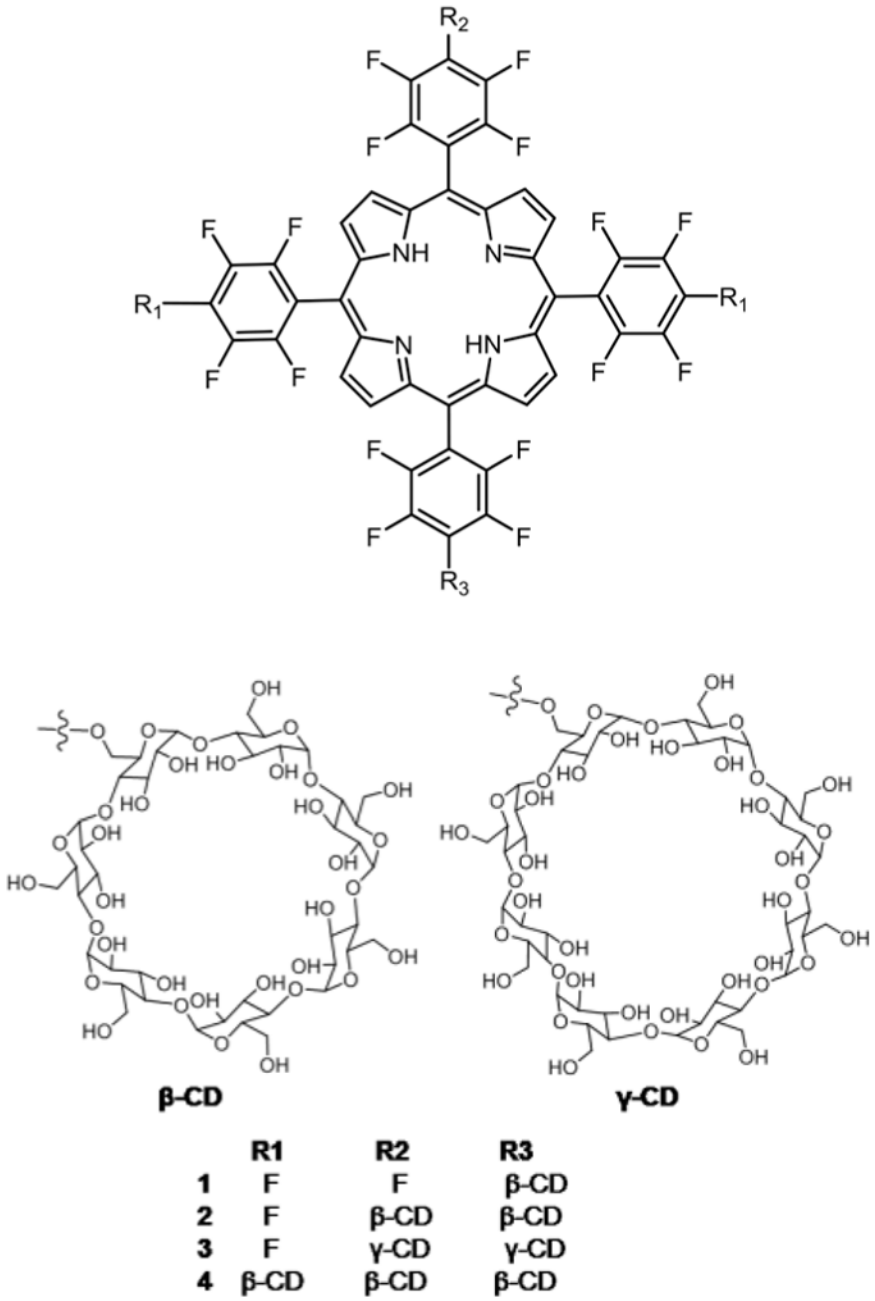

	R1	R2	R3
1	F	F	β-CD
2	F	β-CD	β-CD
3	F	γ-CD	γ-CD
4	β-CD	β-CD	β-CD

Fig. 9.
Porphyrin–CD conjugates, see ref. 82.

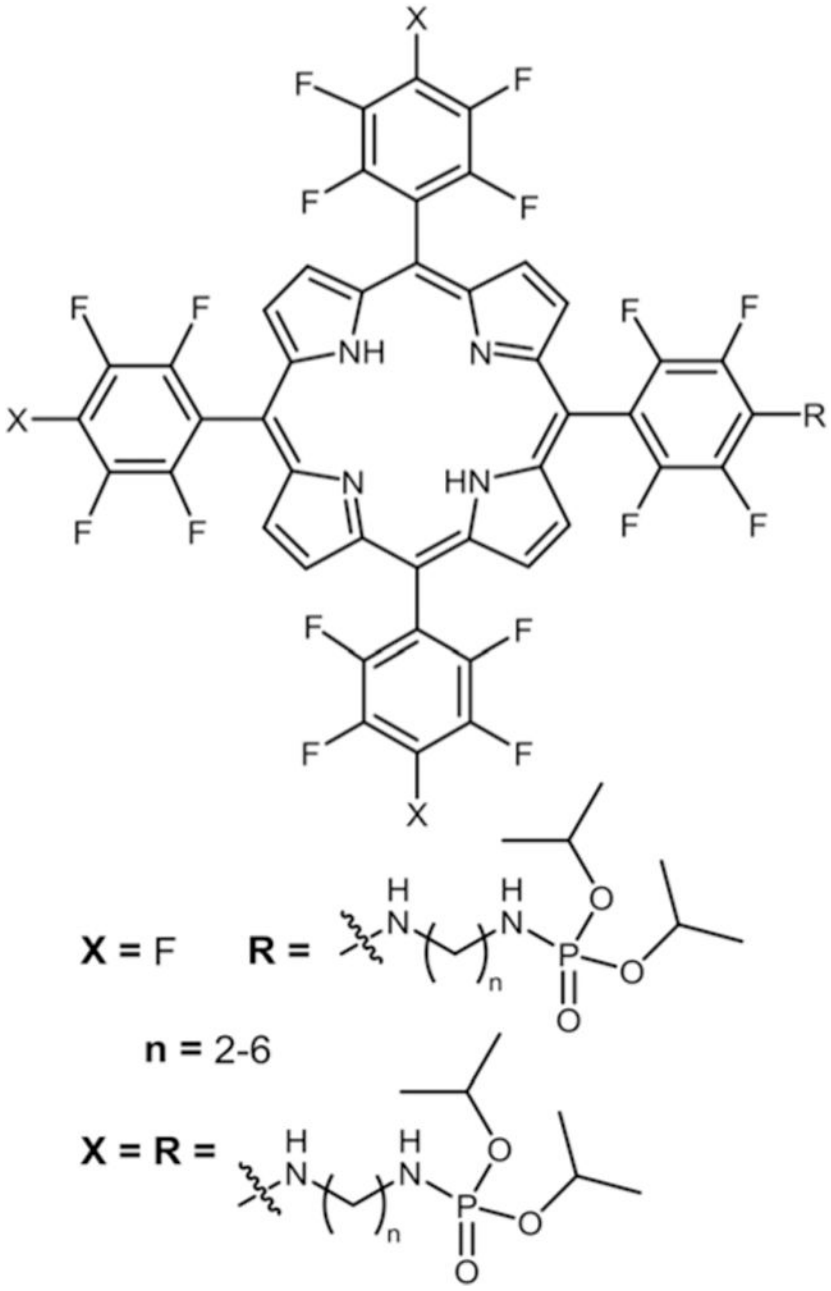

Fig. 10.
Porphyrin–phosphoramidate conjugates, see ref. 83.

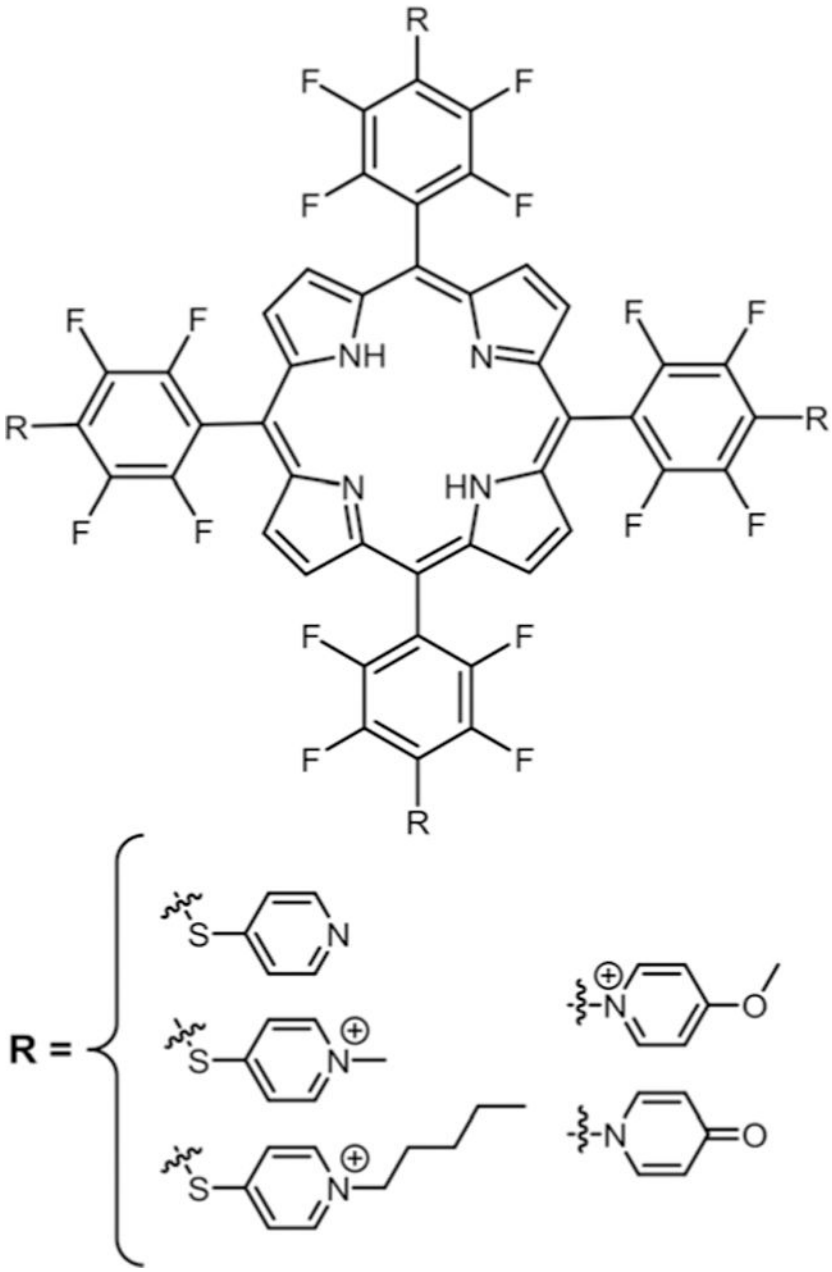

Fig. 11.
Tetra cationic pyridyl porphyrins, see ref. 84 and 85.

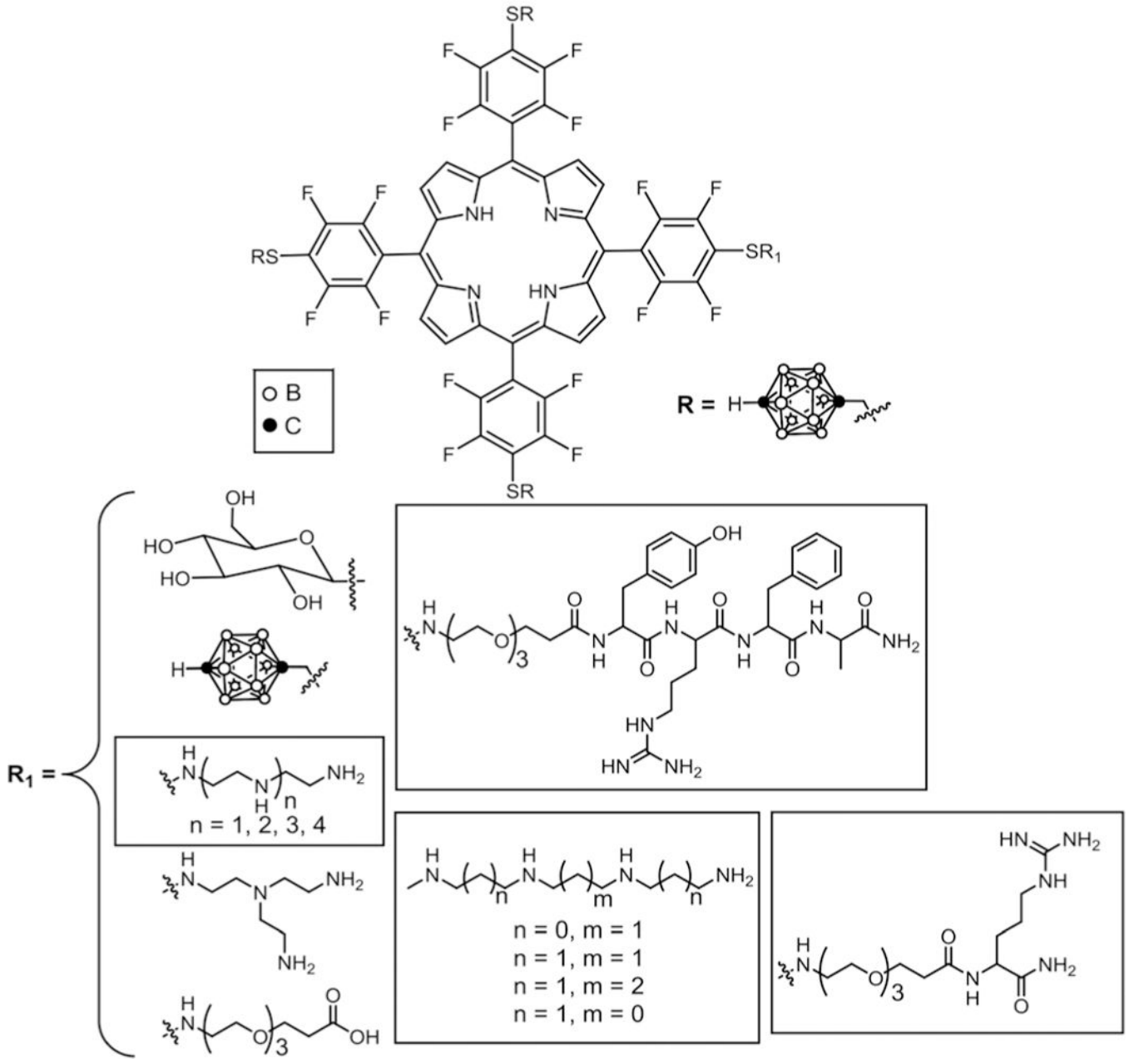

Fig. 12.

Asymmetrical carborane–porphyrin conjugates for BNCT, see ref. 41 and 46.

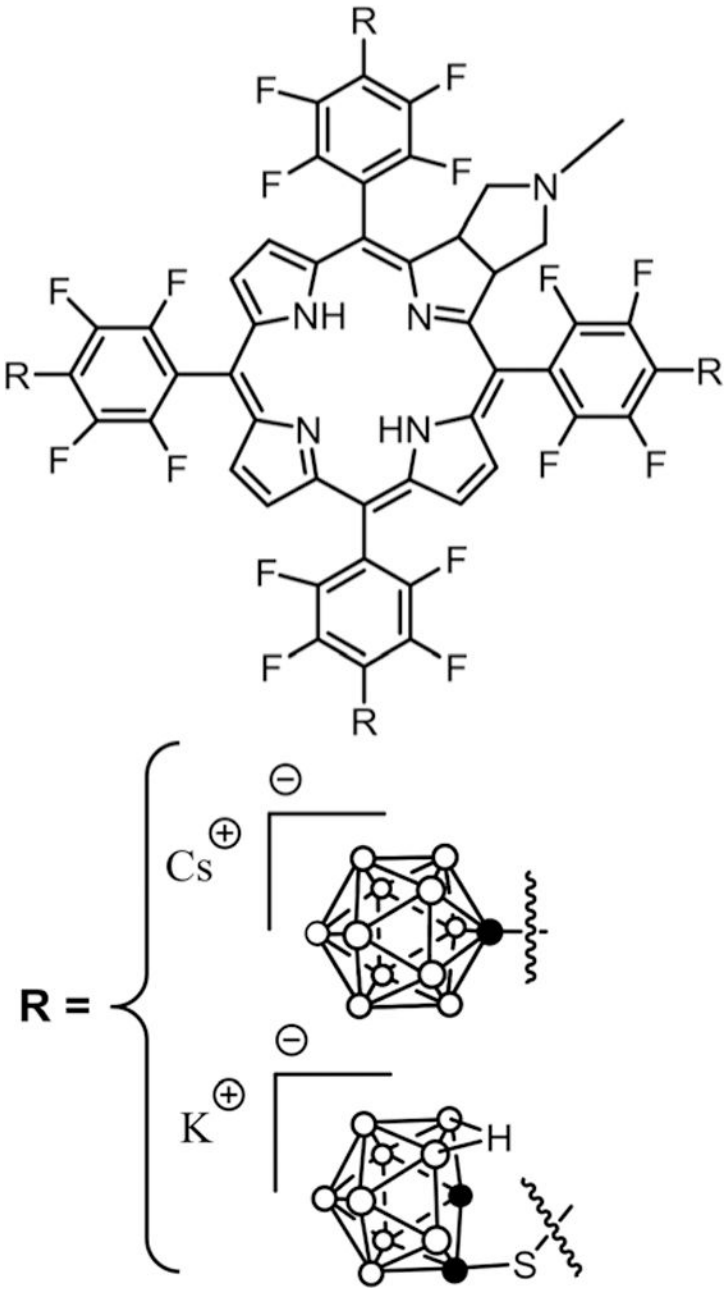

Fig. 13.
Symmetrical tetra substituted carborane–chlorin conjugates, see ref. 68 and 89.

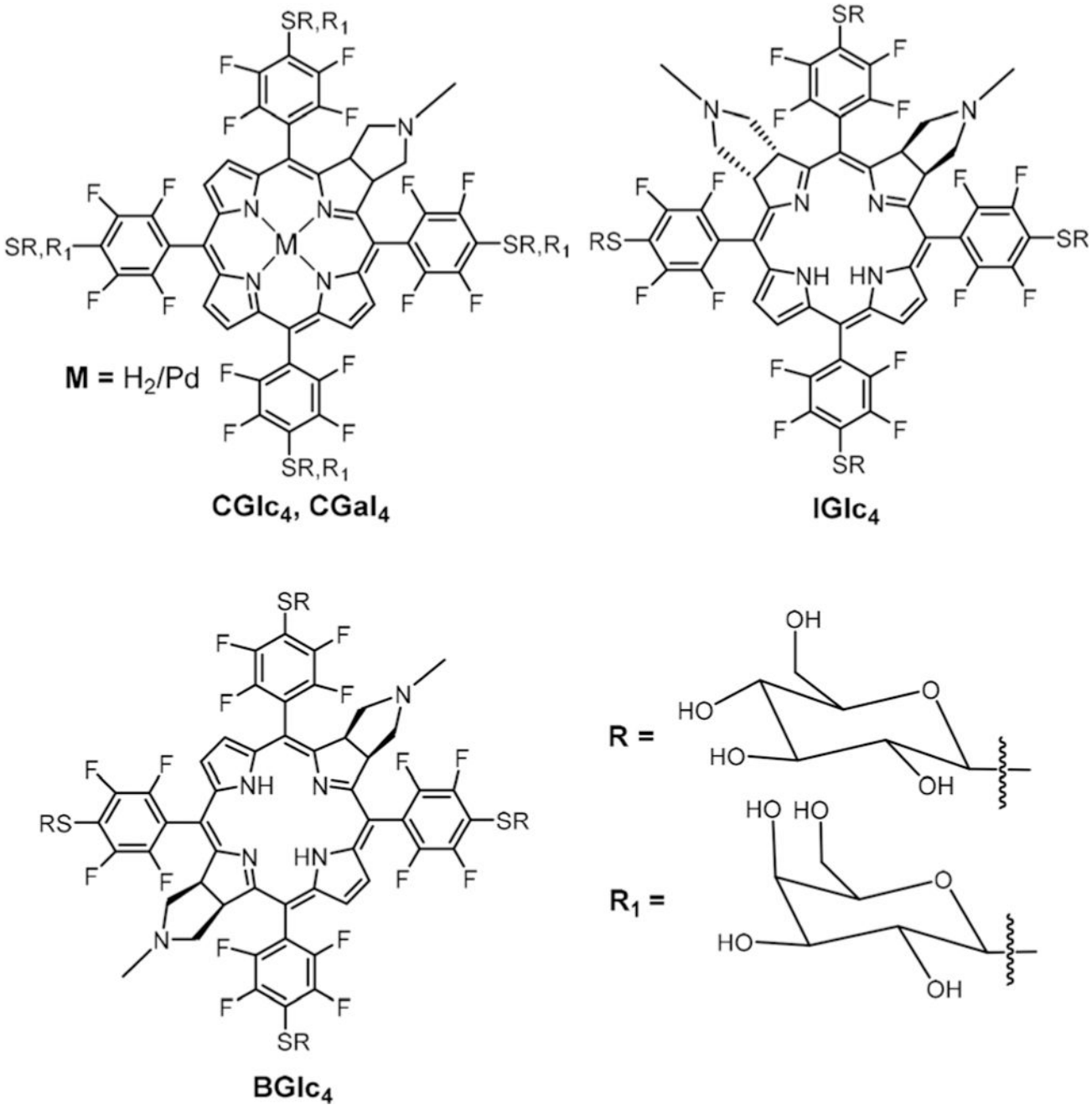

Fig. 14.

Pd and free base $CGlc_4$, free base $CGal_4$, free base $IGlc_4$, and free base $BGlc_4$. See ref. 91, 92, and 94.

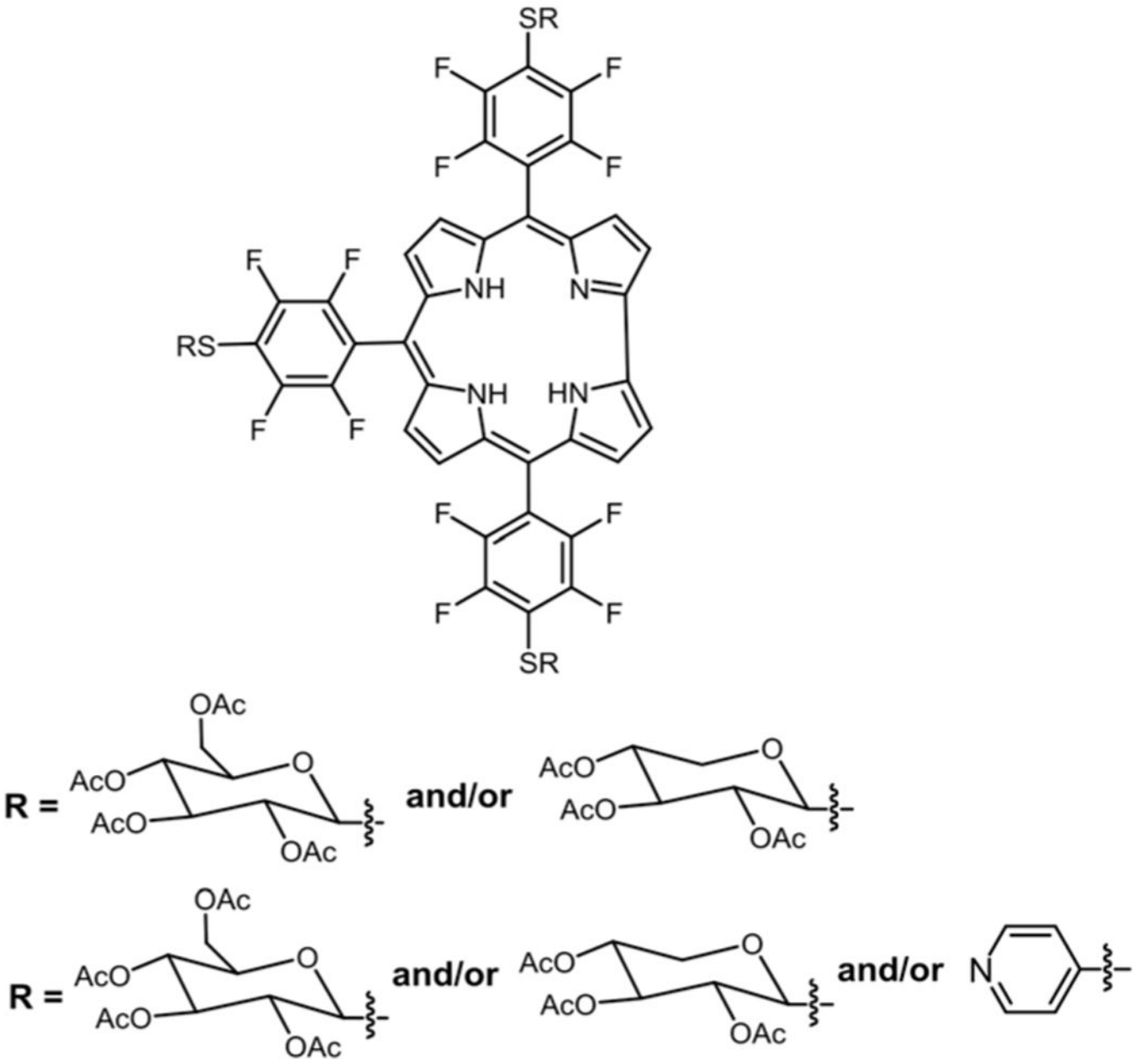

Fig. 15.
Combinatorial library of sugars and pyridyl substituted corroles, see ref. 39 and105.

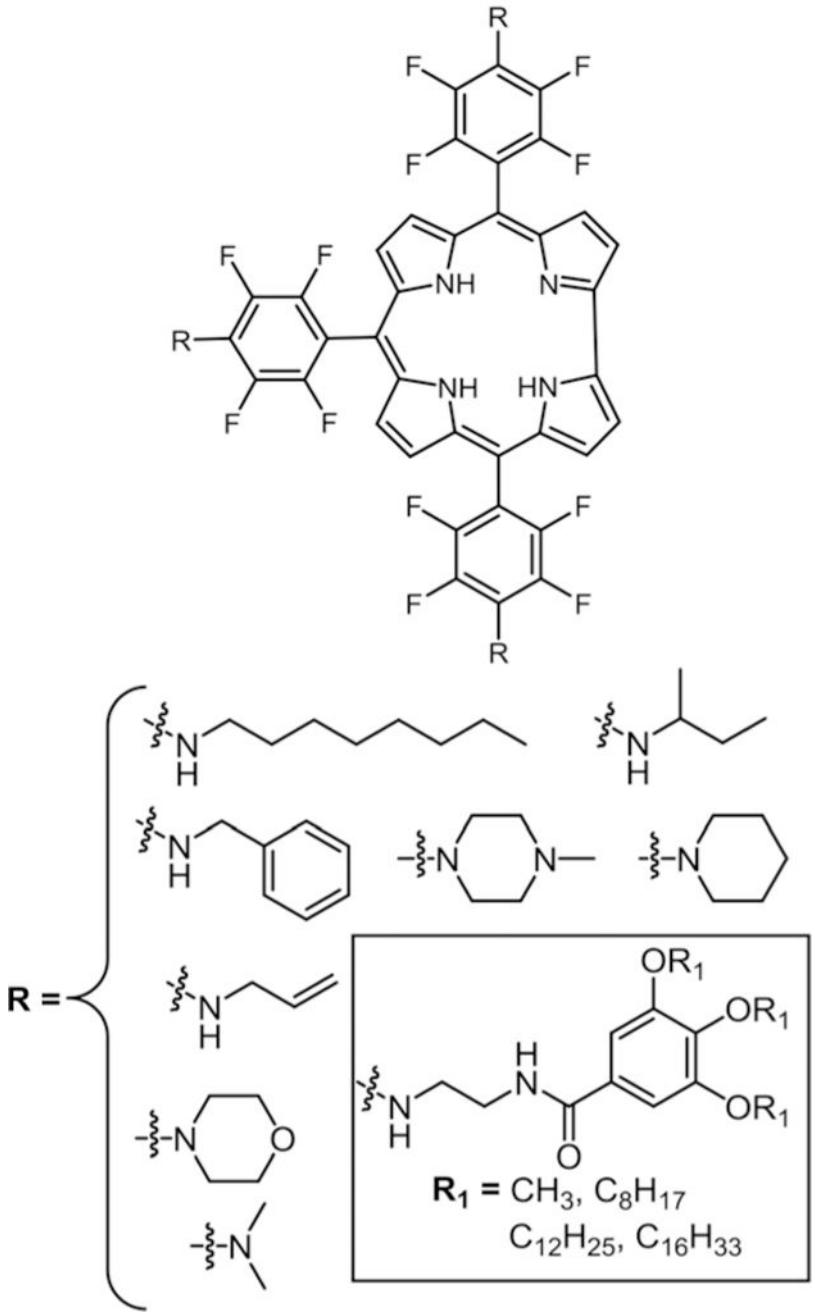

Fig. 16.
Mono and tri amino substituted corrole derivatives, see ref. 106.

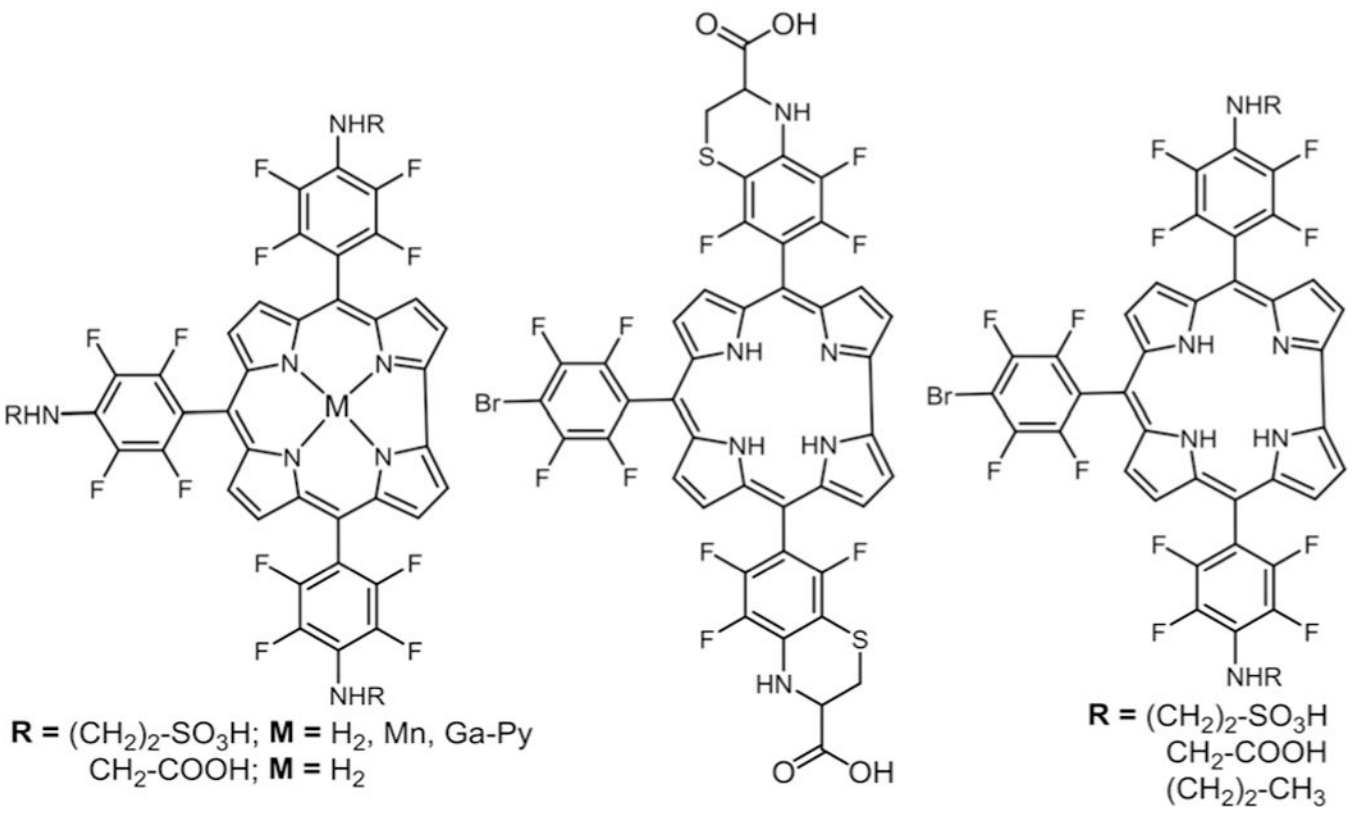

Fig. 17.
Mono and di substituted amino acid-corrole derivatives, see ref.107.

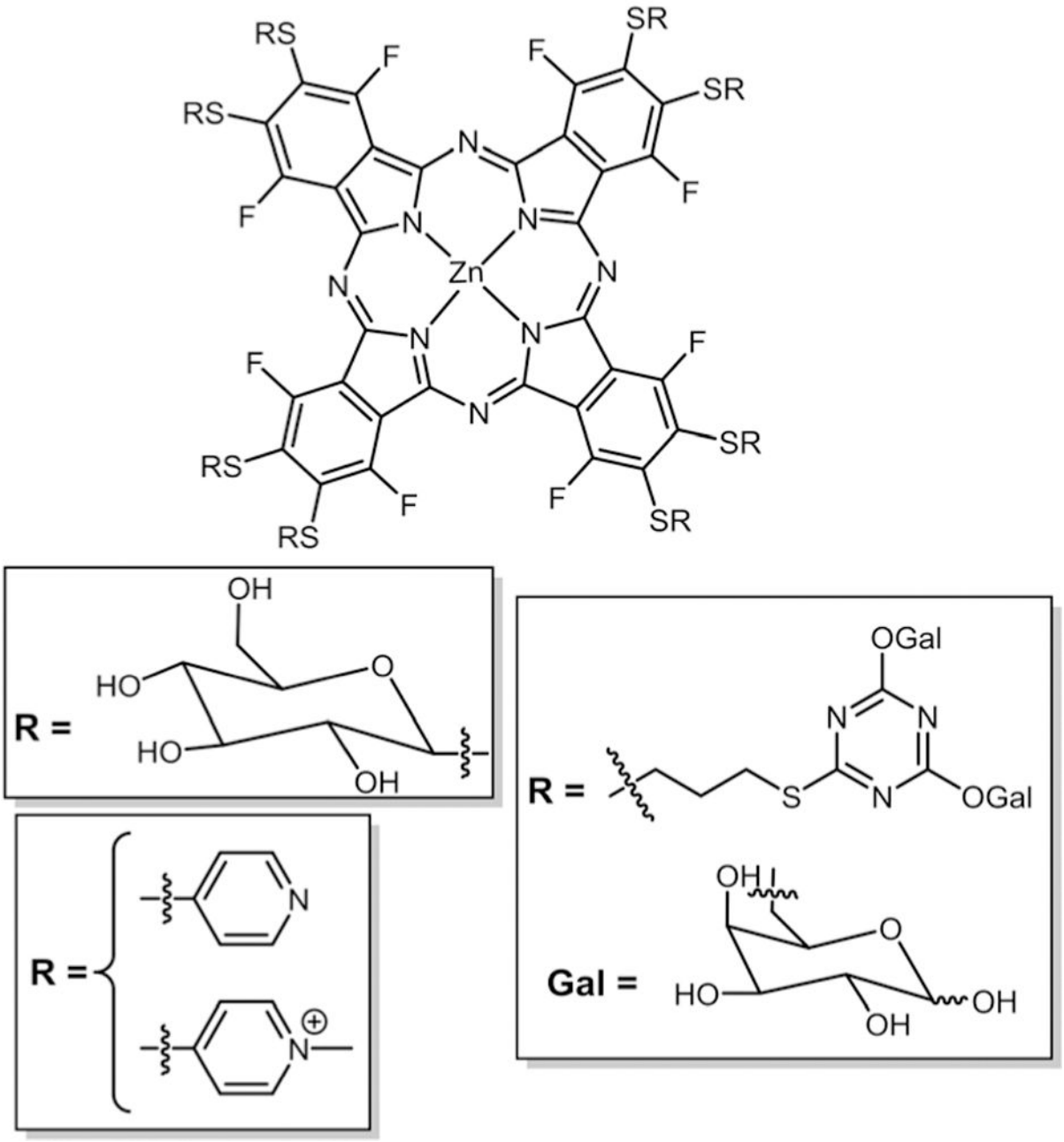

Fig. 18.
Symmetrical octa and hexadecaglycosyl-ZnPc, see ref. 112, 113, and 115.

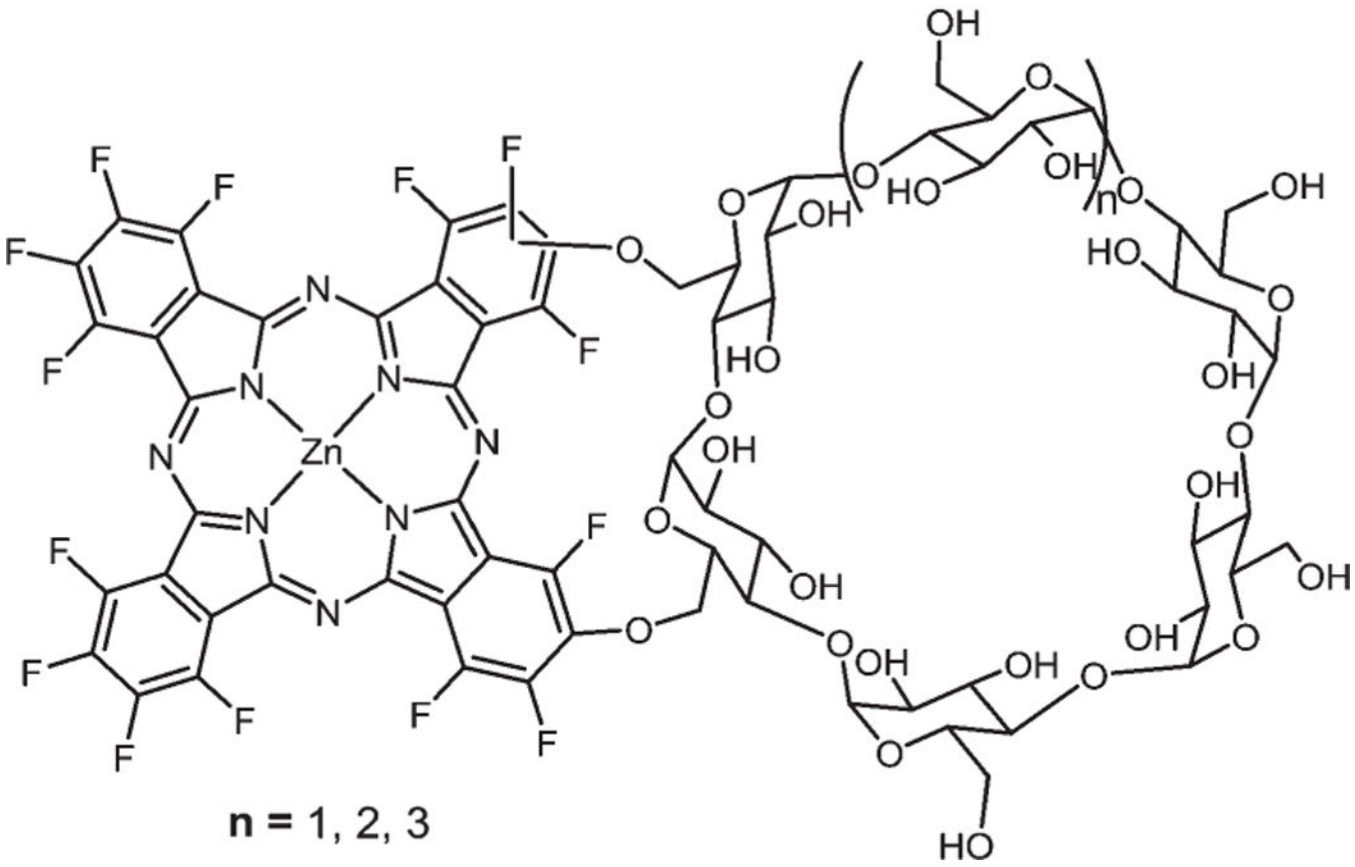

Fig. 19.
Amphiphilic cyclodextrin–Pc conjugates, see ref. 116.

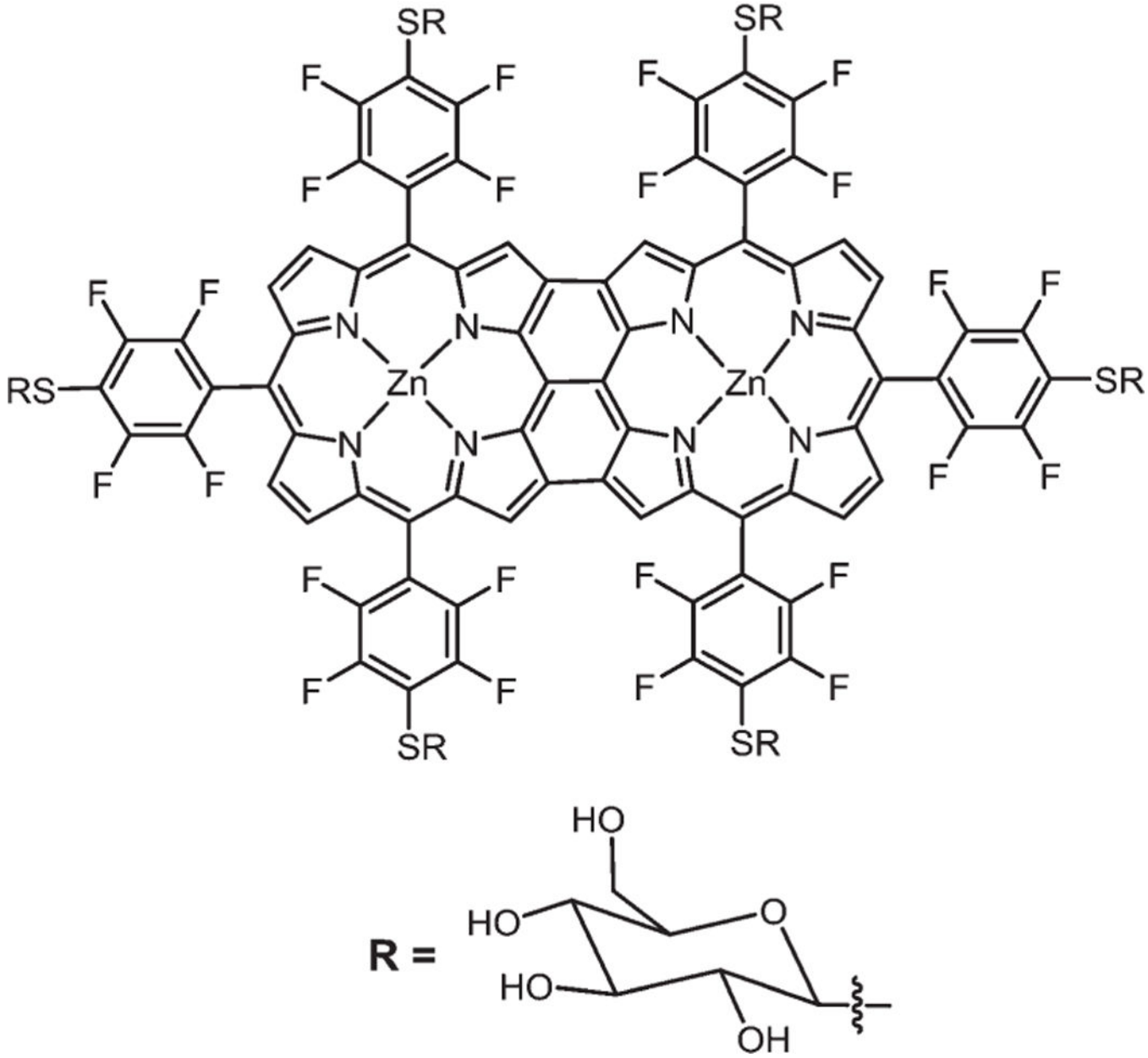

Fig. 20.
Hexathioglucose triply bridged fused porphyrin, see ref. 47.

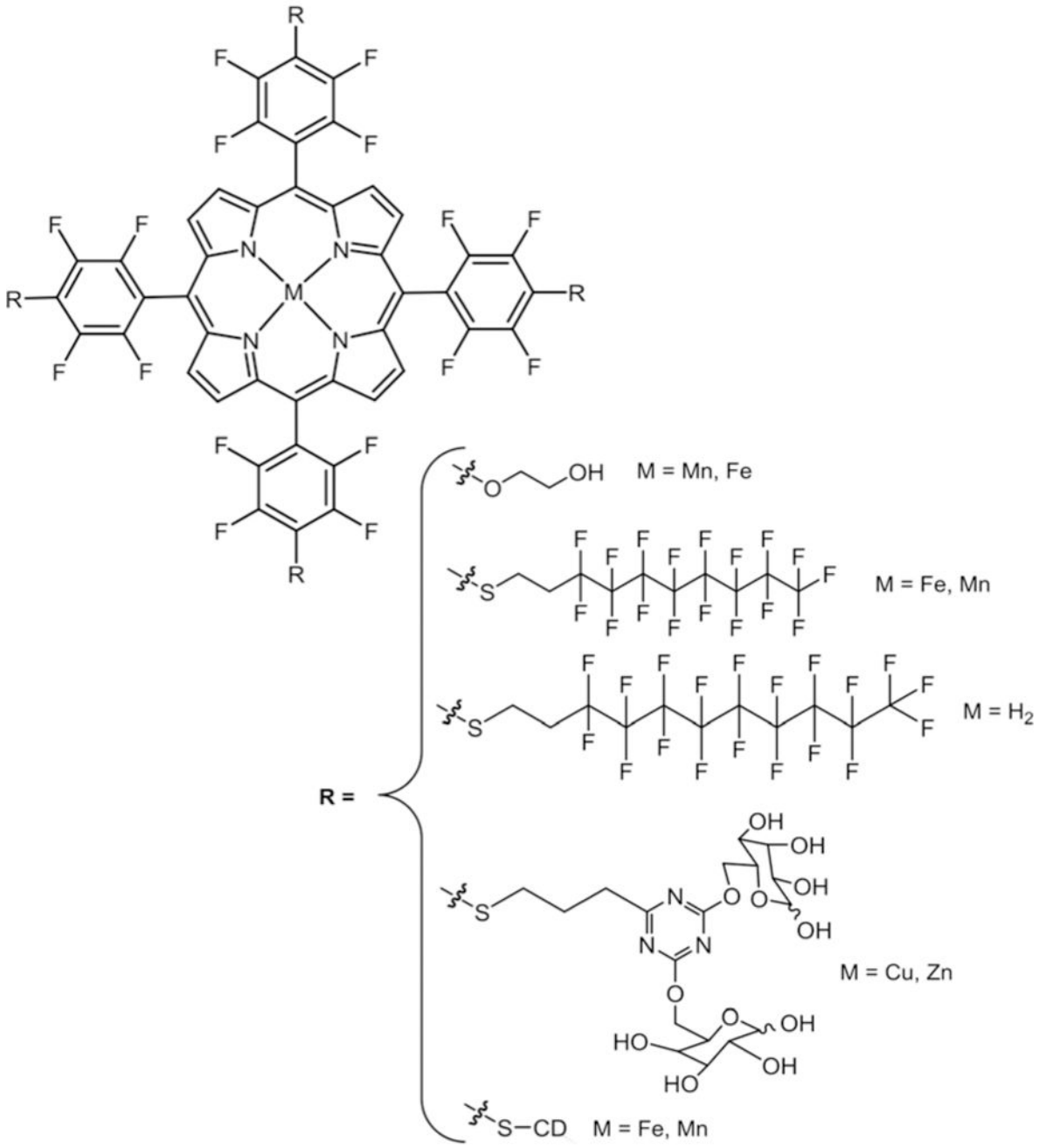

Fig. 21.

Tetra substituted metallated and non-metallated porphyrin thio and oxy derivatives, see ref. 52, 53, 120–122, 124, and 125.

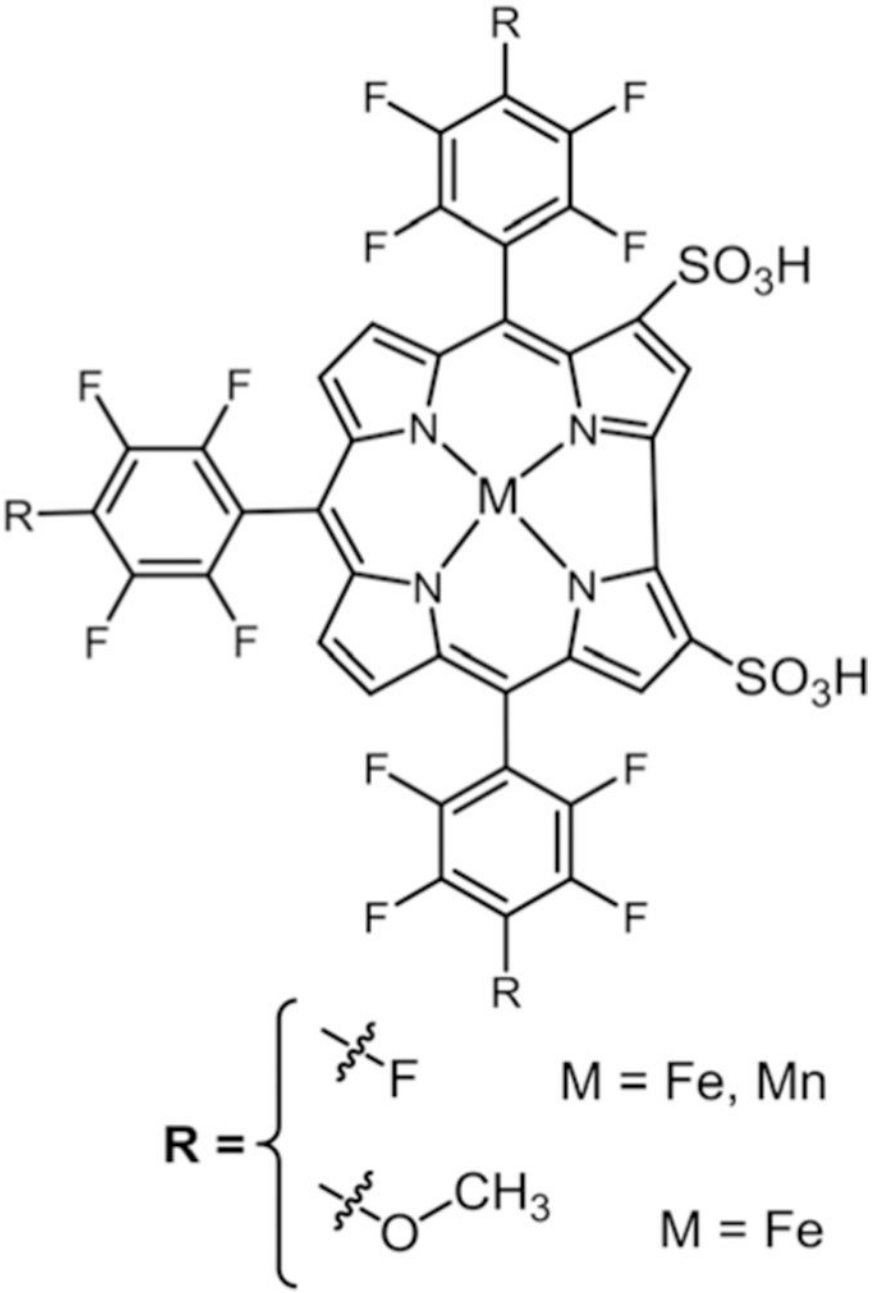

Fig. 22.
Tri methoxy substituted bis-sulfonated corroles, see ref. 134.

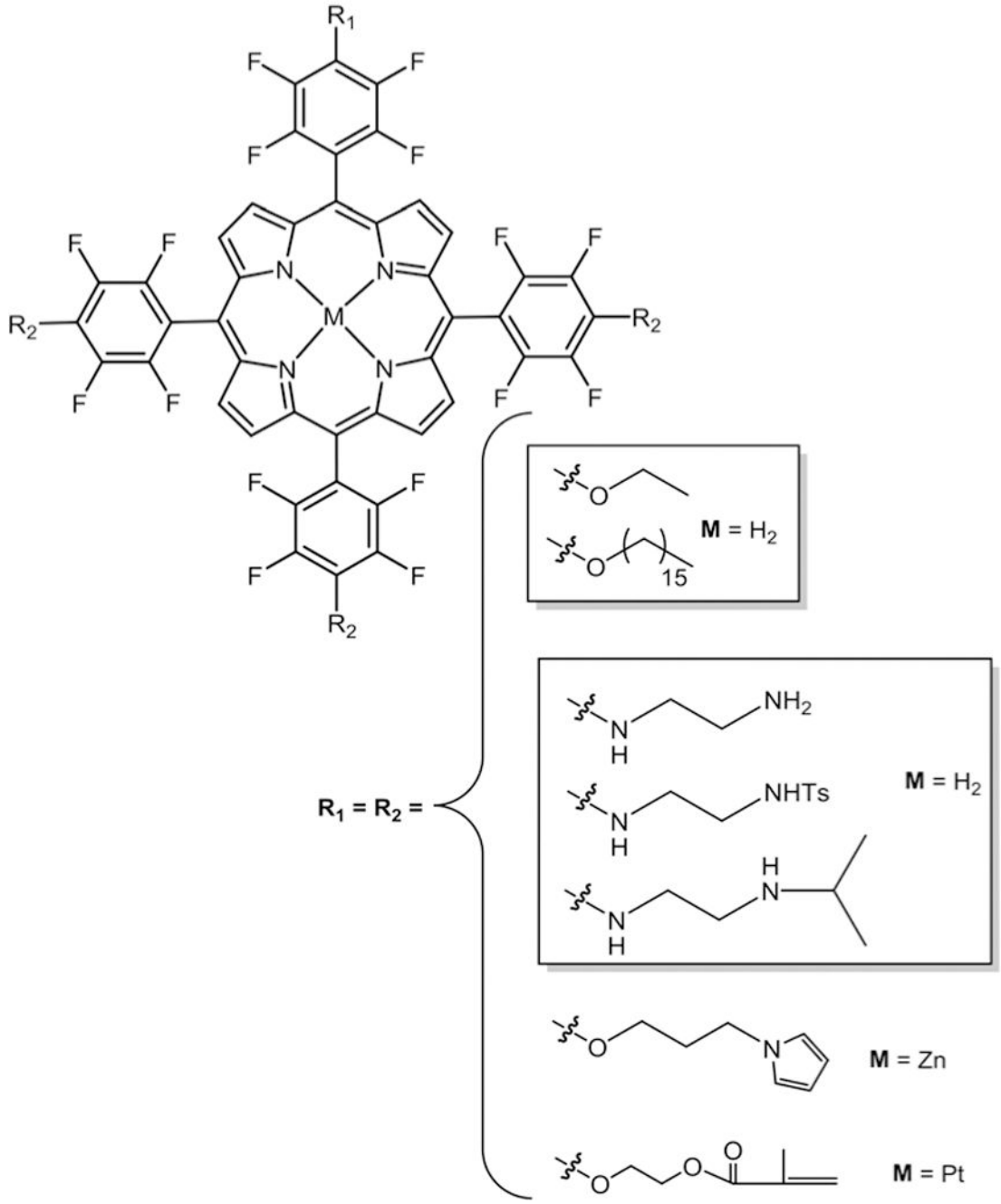

Fig. 23.

Symmetric metallated and free base oxy and amino substituted porphyrin for application as sensors, see ref. 35, 38, 128, and 152.

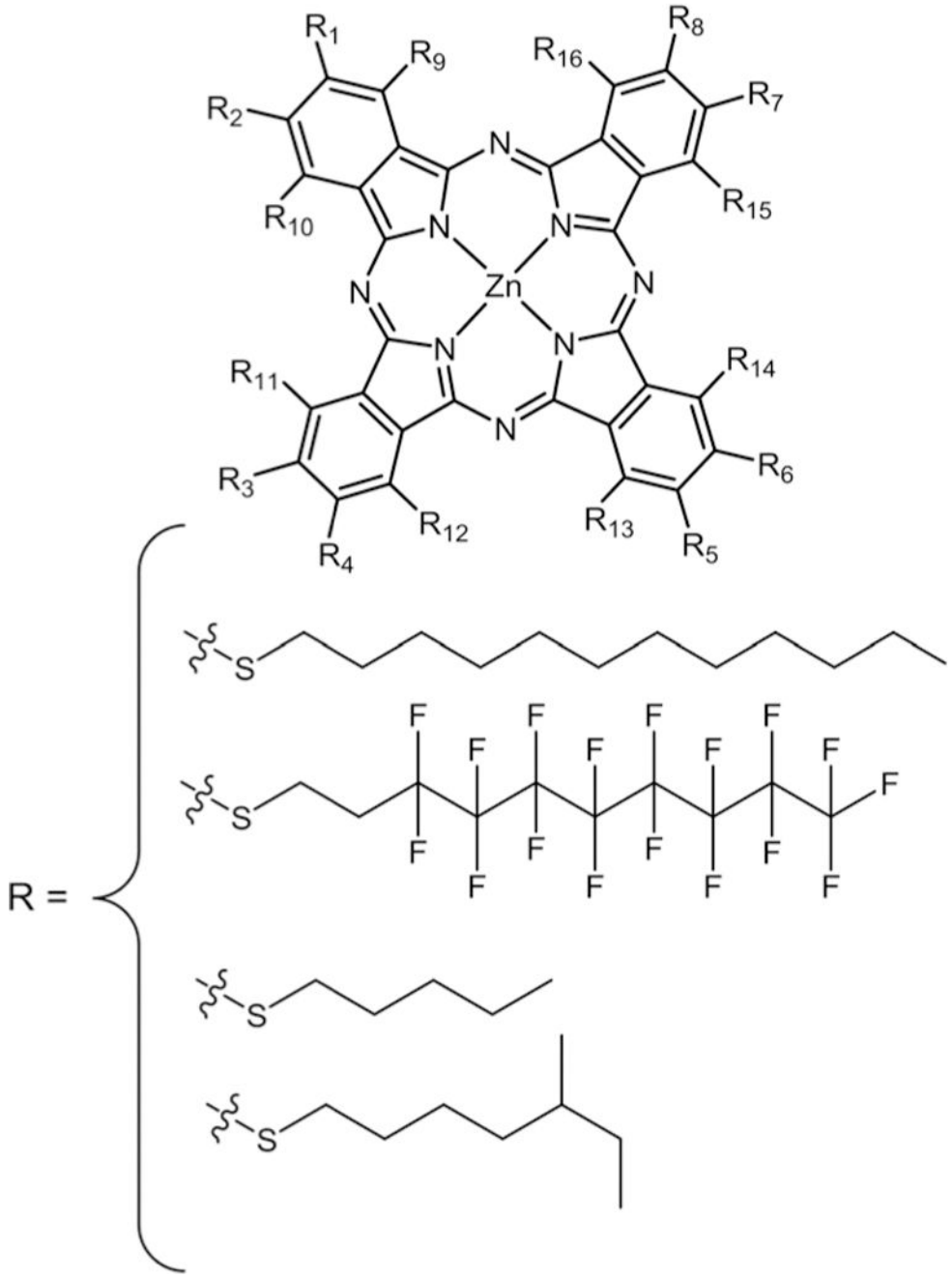

Fig. 24.
Thio substituted phthalocyanines, see ref. 48, 49, and 126.

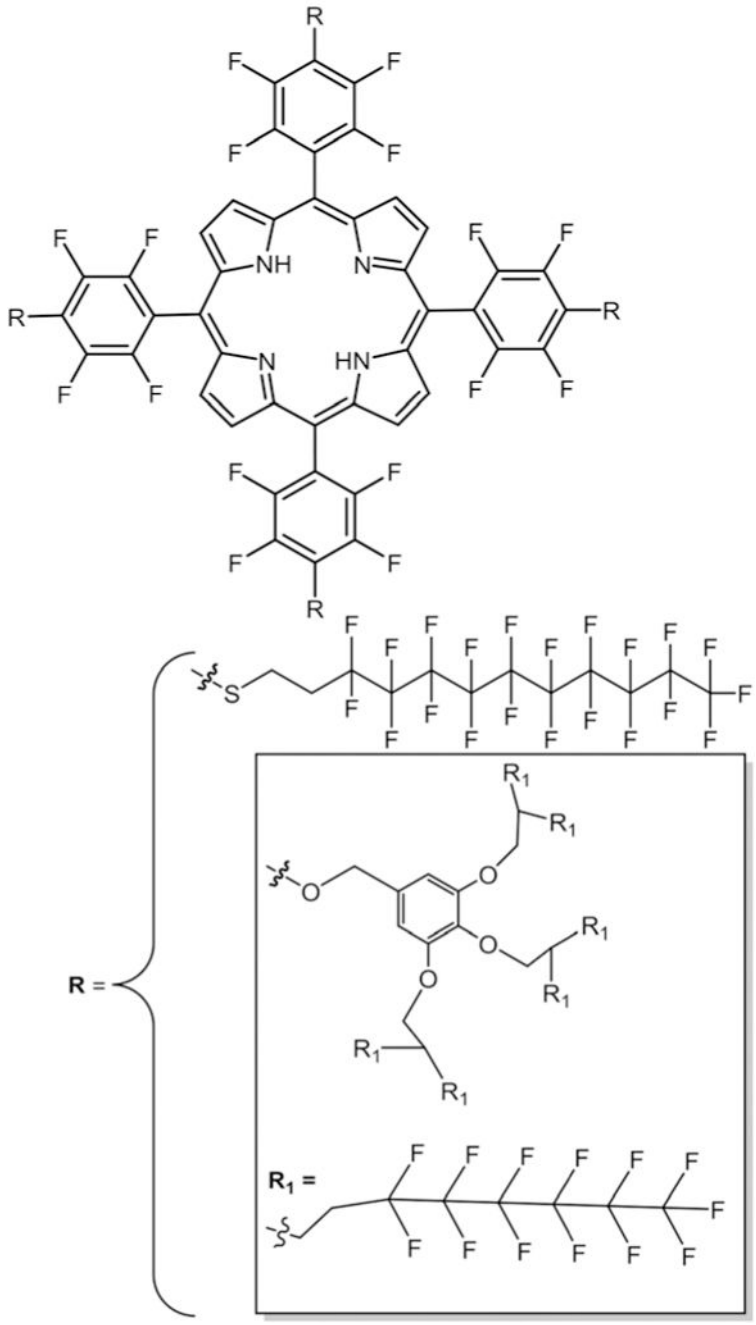

Fig. 25.
Highly fluorinated symmetric porphyrin, see ref. 42 and 176.

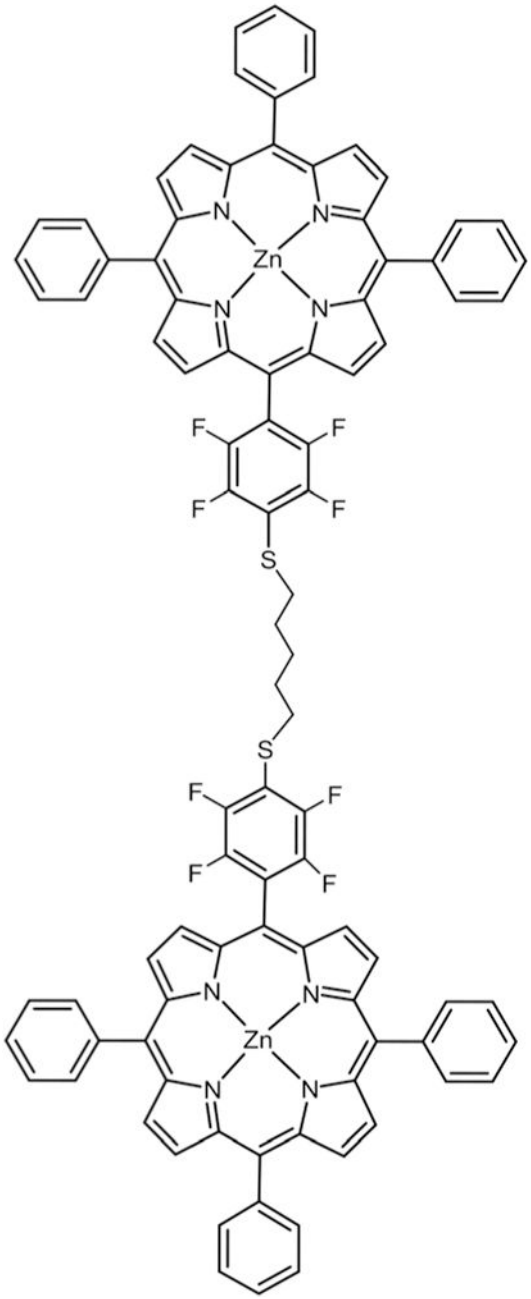

Fig. 26.
Zn porphyrin dimer connected via thio alkyl tether, see ref. 51.

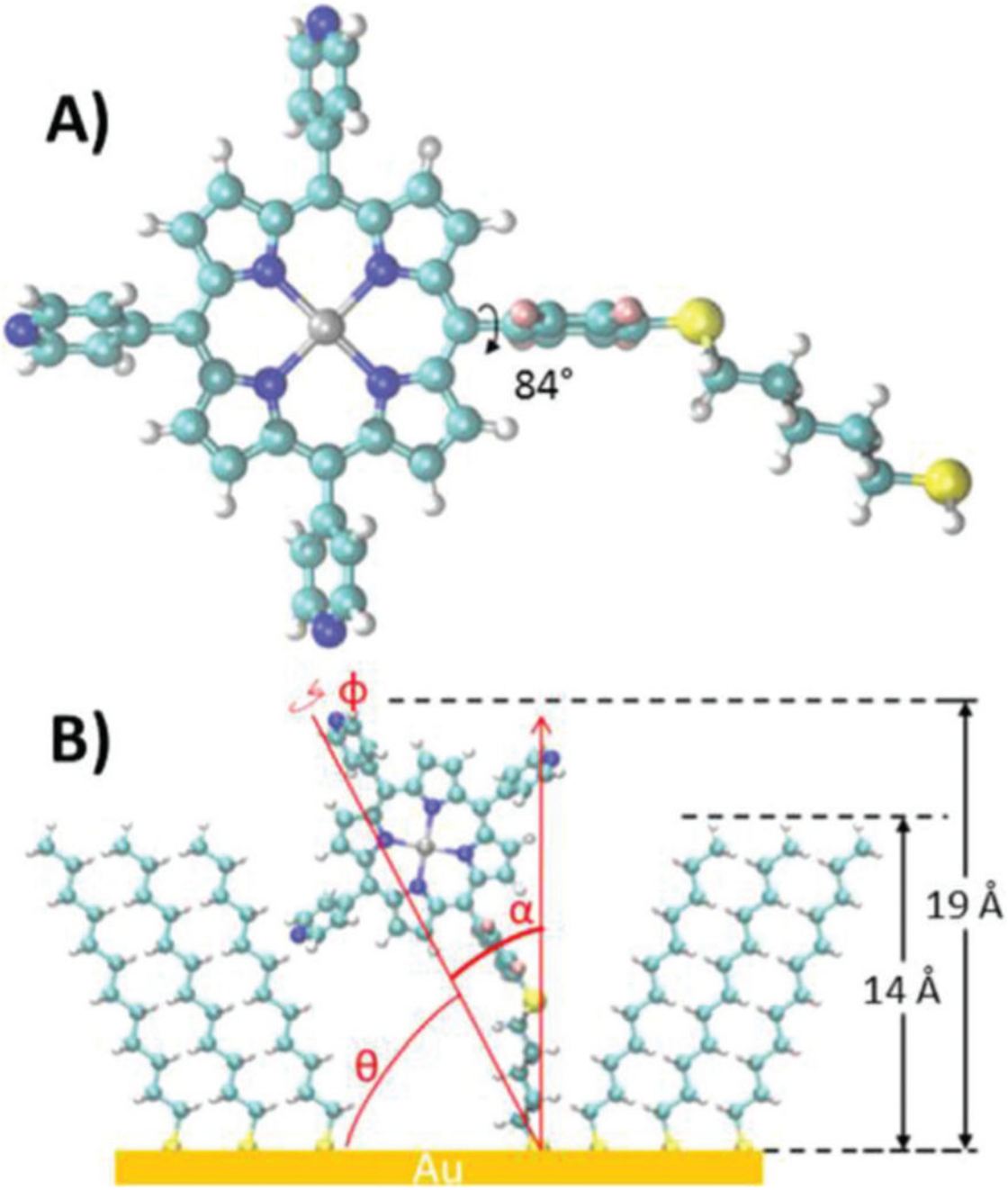

Fig. 27.

(A) Porphyrin molecule with thiol tether (optimized structure from DFT calculations) (Zn or H_2 is grey, carbon is aqua blue, hydrogen is white, nitrogen is blue, fluorine is pink, and sulphur is yellow). (B) Scheme showing the geometry of thioalkyl substituted porphyrin inserting between alkane thiols. See ref. 50 and 177. Reproduced with permission from ref. 50. Copyright 2015 American Chemical Society.